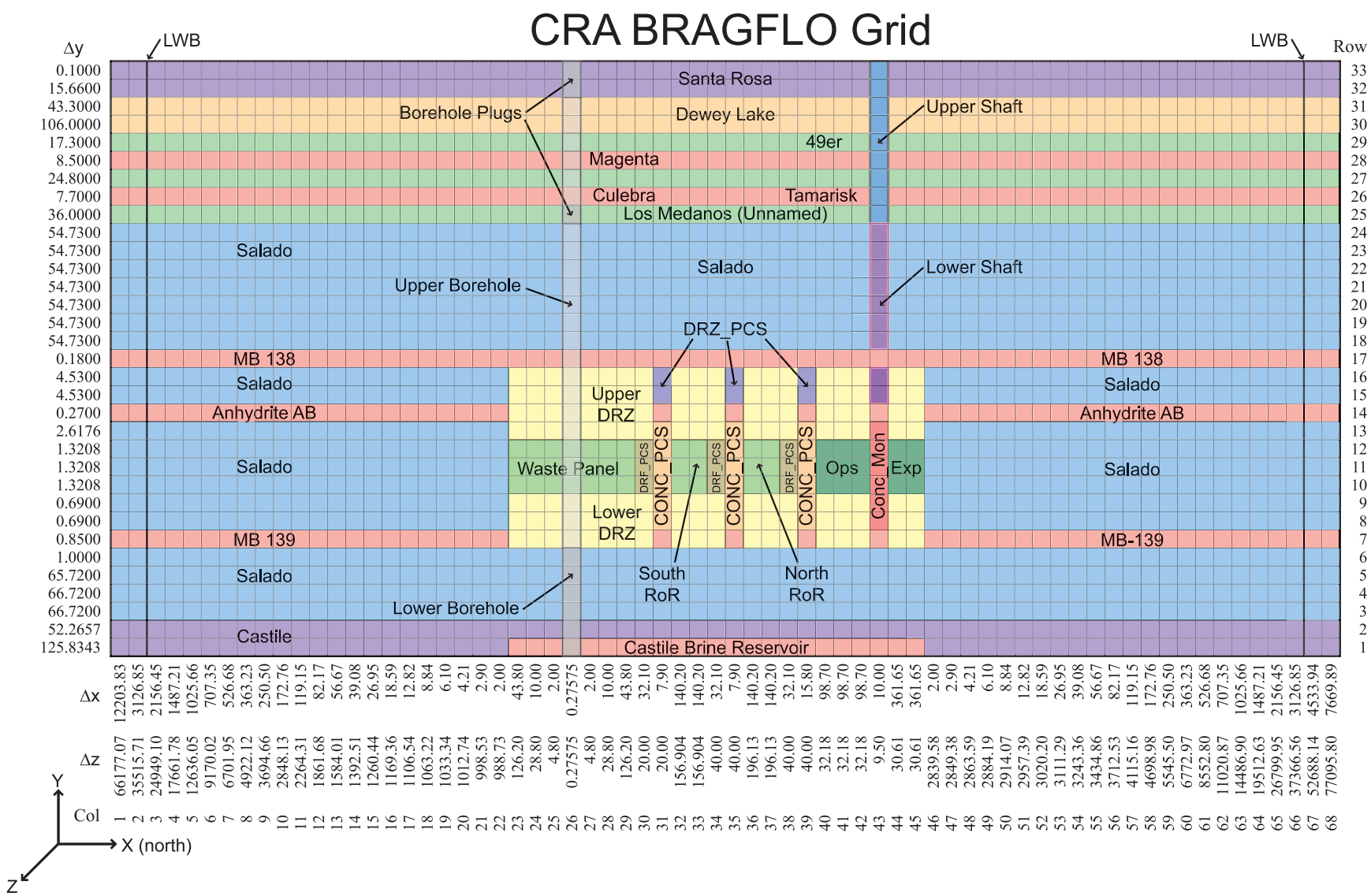

Figure MASS-4. Logical Grid Used for the 2004 PA BRAGFLO Calculations

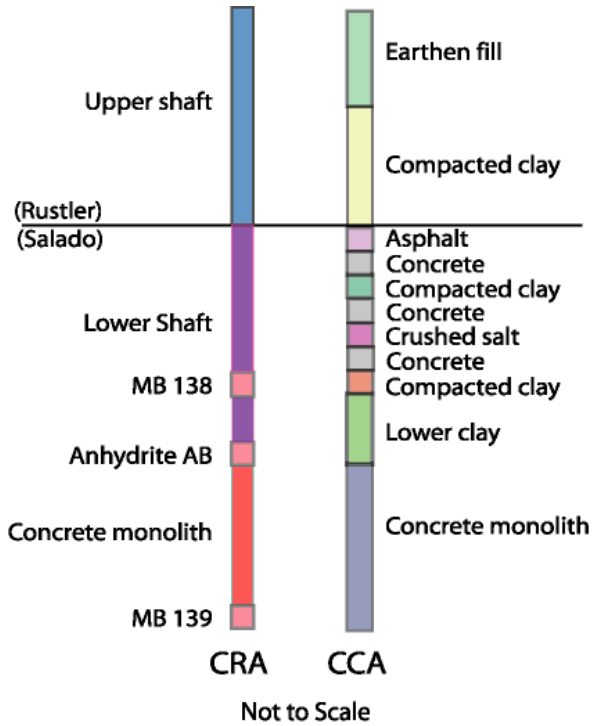

Figure MASS-5. Comparison of the Simplified Shaft (CRA-2004) and the Detailed Shaft (CCA) Models

detailed shaft model in the 1997 PAVT calculations. The conclusion remains that the shaft seals are very effective barriers to flow throughout the 10,000-year regulatory period.

MASS-4.2.3 Implementation of Option D Type Panel Closure

In the CCA, the DOE presented four options for panel closure designs (A through D). Upon reviewing the CCA, the EPA mandated the implementation of the Option D design. For CRA-2004, the true cross-sectional area of the Option D panel closures is represented in the flow model. In addition, to appropriately represent the effect of Option D geometry on repository fluid flow, the segmentation of the waste regions was increased in the grid. This change is described fully in MASS-4.2.4.

For CRA-2004, three sets of panel closures are included in the model domain. The southernmost set of closures represents a pair of closures separating a single waste panel from the other waste areas. The middle set of closures represents four panel closures that will be emplaced between the southern and northern extended panels. The northernmost set of panel closures represents two sets of four panel closures that will be emplaced between the waste regions and the shaft seals.

Each set of panel closures is represented in the CRA-2004 grid with four materials. Refer to Figure MASS-6.

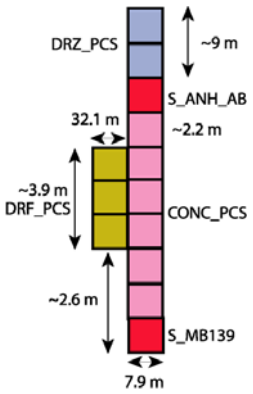

Figure MASS-6. Logical Grid Representation of the Option D Panel Closures for the CRA.

1. ***CONC_PCS: This material represents the concrete monolith, which has properties of SMC.***

2. ***DRZ_PCS: This material represents the DRZ immediately above the concrete monolith that is expected to heal after the emplacement of the monolith.***

3. ***DRF_PCS: This material represents the empty drift and explosion wall portion of the panel closure. This material has the same properties as WAS_AREA (including creep closure).***

4. ***Marker bed materials: These materials are the same as those used to represent the anhydrite marker beds in other parts of the grid. Marker bed materials were used because they have permeability ranges very close to the material CONC_PCS and in the case when pressures near the panel closures exceed the fracture initiation pressure of the marker beds, fractures could extend around the concrete monolith out of the 2-D plane represented by the numerical grid. By using marker bed materials to represent the parts of the panel closures that intersect marker beds, both the permeability of the closure and the potential fracture behavior of marker bed material near the closures are represented.***

Figure MASS-7 is a schematic diagram comparing the panel closure implementation in the CCA and CRA-2004 grids. Permeability ranges are indicated for all materials. Figure MASS-6 shows the 13 grid cells used to represent each set of Option D panel closures in the CRA-2004 BRAGFLO grid.

MASS-4.2.4 Increased Segmentation of Waste Regions in Grid

The CCA/PAVT grid divided the waste regions into two regions; a single panel in the southern end of the repository referred to as the Waste Panel, and a larger region containing the other nine panels referred to as the RoR. The Waste Panel is intersected by an intrusion borehole and is used to represent conditions in any panel that is intersected by a borehole. It is assumed that the Option D panel closures are effective at impeding flow between panels. Therefore, it was considered necessary to divide the RoR into northern and southern blocks

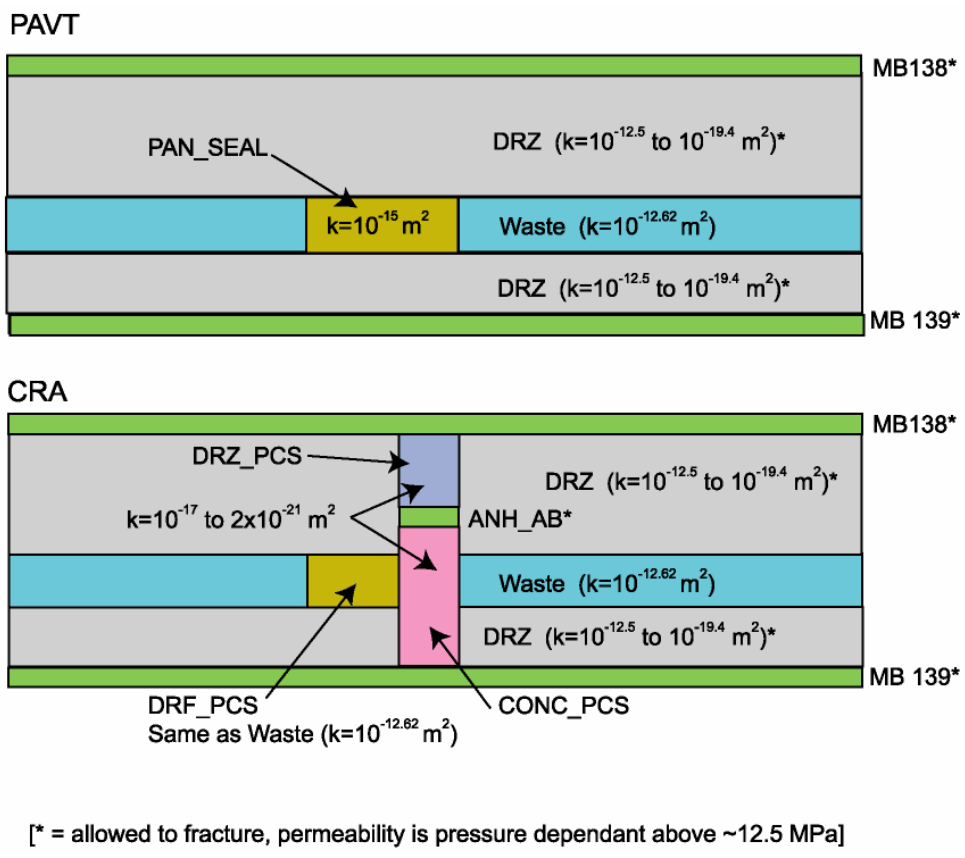

[* = allowed to fracture, permeability is pressure dependant above ~12.5 MPa]

Figure MASS-7. Schematic Comparison of the Representation of Panel Closures in the PAVT and CRA-2004.

separated by a set of panel closures. The south RoR block represents conditions in a panel directly adjacent to an intruded panel. The north RoR block represents conditions in a nonadjacent panel far from the intruded panel (has at least two panel closures between it and the intruded panel). This representation assumes that the effects of drilling intrusions will be damped in nonintruded panels and the degree of damping will depend on the proximity of the drilling intrusion and the number of panel closures separating the intruded panel from other regions of the repository. The delta Z dimensions of the RoR blocks were chosen so that the volume of the southern and northern RoR blocks were equivalent to four and five panels, respectively.

It should be noted that the total volume of the waste-filled areas represented in the CCA/PAVT grid (approximately 4.36×10^5 m^3) was found to be approximately 0.5 percent less than the designed volume (approximately 4.38×10^5 m^3) (Stein 2002). For CRA-2004, the larger correct volume has been used.

MASS-4.2.5 Redefined and Simplified Grid Flaring Method

Grid flaring is a method to represent 3-D volumes in a 2-D grid. Flaring is used when flows can be represented as divergent and convergent from the center of flaring. The CCA/PAVT grid used flaring at two different scales: locally around the borehole and shaft, and regionally

to the north and south of the excavated regions (around a point in the northern end of the RoR). For CRA-2004, the local flaring around the borehole is the same as in the CCA/PAVT grid. The local flaring around the shaft has been eliminated because it has been demonstrated not to be a release pathway. Likewise, the manner in which the regional flaring is calculated has been simplified.

The regional rectangular flaring occurs only for the grid blocks to the north and south of the excavated region. The CRA flaring is very similar to what was done for the CCA/PAVT grid; however the CRA flaring methodology is easier to implement. To define the flaring, it is assumed that looking from the top of the grid (x-z plane), the excavated regions of the grid can be approximated by a rectangle with length equal to the distance between the southern edge of the Waste Panel and the northern edge of the Experimental Area in the grid (x = 1830 m) and width, defined so that the area of the rectangle is equal to the total area of the excavated regions of the grid in the x-z plane (z = 80 m). In order to calculate the rectangular flaring for the grid cells outside the excavated regions, a centerline is defined to divides the flaring on the north and south. Because the waste panels are located in the southern part of the excavated area, the centerline is chosen to be the "center of waste" as the middle of the panel closure that separates the northern RoR from the southern RoR. The position of this center of the waste is described as the distances from the north and south edges of the gridded repository, DN and DS, respectively {DN = 1378 m, DS = 452 m, DN + DS = 1830 m}. Each flared grid block has length, Dx, and width, Dz. The block can be thought of as wrapped around the excavated area like half a rectangular onion, with the center at the center of waste (Figure MASS-8). Each Dz can be calculated from the preceding Dxs as follows.

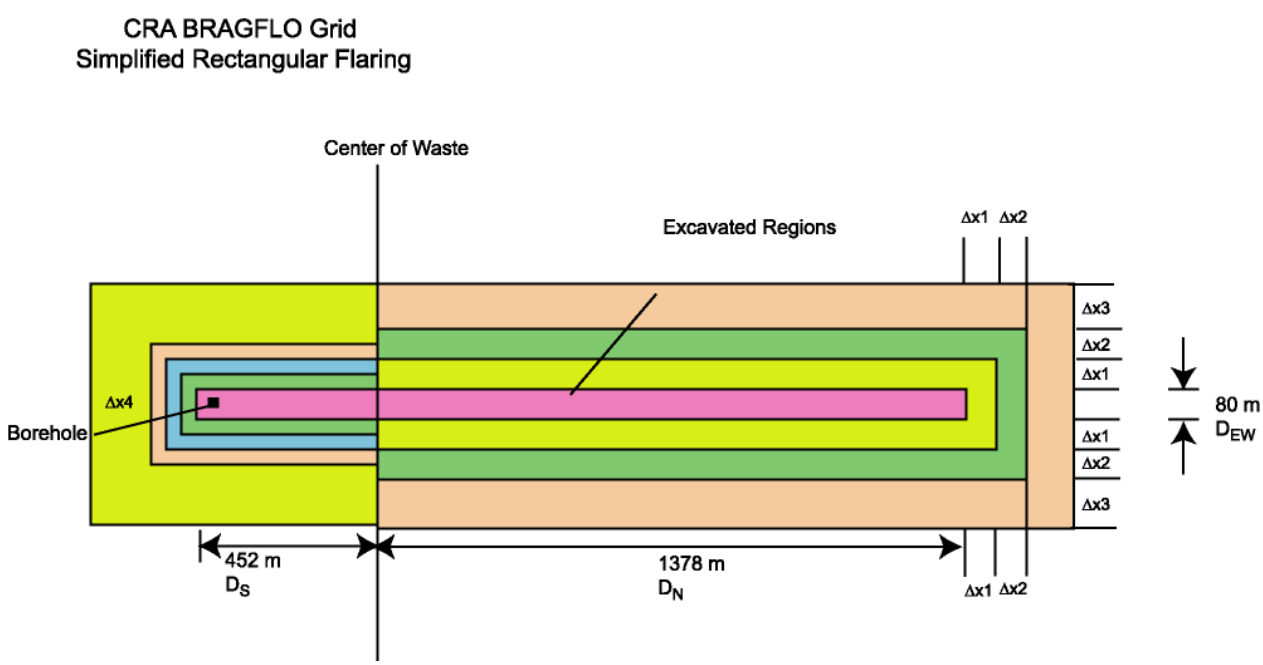

Figure MASS-8. CRA Flaring

For the northern end:

$$\Delta z_1 = 2D_N + D_{EW} + 2\Delta x_1$$
$$\Delta z_2 = 2D_N + D_{EW} + 4\Delta x_1 + 2\Delta x_2$$
$$\Delta z_3 = 2D_N + D_{EW} + 4\Delta x_1 + 4\Delta x_2 + 2\Delta x_3$$

Flaring for blocks wrapped around the southern end is the same with D_S substituted for D_N.

This method of rectangular flaring ensures that the grid accounts for all the volume surrounding the repository.

MASS-4.2.6 Refinement of the X-Spacing Outside the Repository

The grid blocks to the north and south of the excavated region will be refined in the x-direction from the baseline grid. The x-dimension of the grid cells immediately to the north and south of the repository start at 2 m and increases by a factor of 1.45. Exceptions to this are

$$\Delta z_n = 2D_N + D_{EW} + 4\sum_{i=1}^{n-1} \Delta x_i + 2\Delta x_n$$

made to ensure that the location of the Land Withdrawal Boundary (LWB) and the total extent of the grid matches that in the baseline grid. This refinement factor was chosen to reduce numerical dispersion caused by rapid increases in cell dimensions (Anderson and Woessner 1992; Wang and Anderson 1982).

MASS-4.2.7 Refinement of the Y-Spacing

In the y-direction, the grid spacing within layers representing the Salado has been changed from the CCA/PAVT. The CCA grid spacing in the Salado was dictated by the thickness of different shaft seal materials. Since the shaft is no longer represented in the model domain, the y spacing in the Salado is now uniform. In addition, two layers were added immediately above and below MB 139 to refine the grid spacing and reduce numerical dispersion. These changes result in a total of 33 y-divisions for the grid, and will increase the numerical accuracy of flow and transport calculations.

~~The geometry used in the disposal-system model has seen numerous changes since the 1991 preliminary performance assessment (WIPP Performance Assessment Division 1991), in which undisturbed performance used different geometrical assumptions than for disturbed performance, but all calculations used homogeneous waste regions. In gas and brine migration calculations performed in 1992 prior to the 1992 performance assessment for 40 CFR Part 191 (WIPP Performance Assessment Department 1992a) several different geometries were again used, however some of these explored discretizing the repository into different waste and panel seal regions and explored the impact of the north end of the repository. The 1992 performance assessment calculations used geometries similar in principle to those used for the 1992 gas and brine migration calculations (Sandia WIPP Project 1992; WIPP Performance Assessment Department 1992b).~~

~~The current disposal system geometry was chosen to allow simulations for both disturbed and undisturbed scenarios to use the same grid description. The repository regions that contain waste have been divided into two subregions: a panel region and the remainder of the repository. Separating the panel region allows a more detailed representation of an intrusion borehole penetrating a panel. The effects of inter-panel communication can be examined by varying the permeability of the panel closure. In addition, the Culebra and other geologic units extending to the surface are represented. The various shaft seal components are also included in the modeling. The computational grid used in BRAGFLO is identical for all three scenarios, and the distinction between scenarios is facilitated by introducing material changes at specified time intervals. For example, at the time of an intrusion the material properties corresponding to the borehole grid blocks are changed to those properties consistent with the long-term behavior of a borehole and plug system.~~

~~MASS.4.3 Historical Context of Culebra Geometries as Modeled in SECOFL2D and SECOTP2D~~

~~The geometries used in the SECOFL2D and SECOTP2D Culebra models are chosen to provide a reasonable and realistic basis for two-dimensional simulations of groundwater flow and radionuclide transport through the Culebra. This model, described in Sections 6.4.2 and 6.4.6.2, has been developed over many years. The development of the various modeling domains and assumptions is documented in Section MASS.15.~~

MASS-5.0 BRAGFLO GEOMETRY OF THE REPOSITORY

~~The purpose of this model is to provide a reasonable representation of the geometry of the WIPP repository with respect to the interactions between important processes that occur there.~~

~~This conceptual model represents the geometry of the repository for performance assessment.~~ ***The repository geometry conceptual model is represented using the BRAGFLO code.*** As with the geometry of the disposal system discussed in Section~~s~~ 6.4.2.1~~)~~ and ~~Section MASS.4~~***earlier in this section***, the principal process considered in setting up the repository geometry is fluid flow. Several features considered to be important in fluid flow are included in the conceptual model. The first is the overall dimension of the repository along the north-south trend of the cross section, as well as the major divisions within the repository (waste disposal region, operations region, and experimental region). The second is the volume of a single panel, because fluid flow to a borehole penetrating the repository can potentially access only the volume in a waste panel directly and other regions of the repository only by flow through or around a panel closure. The third is the physical dimensions of panel closures separating the single panel and the other major divisions of the repository. ~~In determining the appropriate way to represent these features, the important concepts applied are to preserve dimensions along the axis of the model, interface areas, and volumes excavated.~~

Notably absent from the conceptual model for the long-term performance of the repository are pillars and individual drifts and rooms. These are excluded from the model for simplicity, and it is assumed that they have either negligible impact on fluid flow processes or, alternatively, that including them in the conceptual model would be beneficial to long-term performance because

their presence could make flow paths more tortuous and decrease fluxes. This assumption includes lumping ***four and five*** ~~nine~~ of the 10 panels in***to*** the ***south RoR and north RoR regions respectively (see MASS-4.2.4).*** ~~waste disposal region into a single region (see Sections 6.4.3 and 6.4.3.2).~~

The BRAGFLO model of the WIPP disposal system is a two-dimensional array of three-dimensional grid blocks. Each grid block has a finite length, width, height, volume, and surface area for its boundaries with neighboring grid blocks. The BRAGFLO two-dimensional grid is similar to any other two-dimensional grid used to treat flows, except that the grid-block dimension in the direction perpendicular (z-direction) to the plane of the grid varies from block to block as a function of the lateral direction (x-direction***; see MASS-4.2.5***). This allows the BRAGFLO grid to treat important geometric aspects of the WIPP disposal system, such as the very small intrusion borehole, the moderate-size shaft, and the larger controlled areas. ***The grid configurations used in the 1996 CCA PA and 1997 PAVT are shown in Figure MASS-3 while the 2004 PA grid is shown in Figure MASS-4.***

MASS-5.1 Historical Context of the Repository Model

Several early models of repository fluid-flow behavior (models of radionuclide migration pathways, gas flow from the disposal area to the shaft, Salado brine flow through panel to borehole, effects of anhydrite layers on Salado brine flow through a panel, and flow from a brine reservoir through a disposal room) are summarized in a 1990 report (Rechard et al. 1990). In the preliminary performance assessment of 1992, all waste was lumped into a single region (WIPP Performance Assessment Department 1993). Because human intrusion boreholes ~~must be~~***were*** treated in detail for the 1996 performance assessment, it was necessary to model a single waste panel with a borehole surrounded by two-dimensional radial-flaring gridblocks. ***This approach is continued for the 2004 PA. The 1996 PA treated the*** ~~The~~ remainder of the waste ***area as a single RoR*** ~~is modeled as the rest of therepository~~***. For the 2004 PA, the RoR is divided into two areas separated by a panel closure system. This change was made to more adequately simulate the effects of the Option D closure in impeding fluid flow between panels.*** ~~and is separated from the waste panel by a panel closure.~~

MASS-6.*0* CREEP CLOSURE

The model used for creep closure of the repository is discussed in ***Appendix PA, Attachment PORSURF.*** ~~Appendix PORSURF, Chapter 6.0 (Section 6.4.3.1), and Appendix BRAGFLO (Section~~ 4.11). ***Historical information is contained in CCA Appendix PORSURF.***

MASS-7.*0* REPOSITORY FLUID FLOW

This model represents the long-term flow behavior of liquid and gas in the repository and its interaction with other regions in which fluid flow may occur, such as the Salado, shafts, or intrusion borehole. This model is not used to represent the interaction of fluids in the repository with a borehole during drilling. ***Historical information on alternative conceptual models for brine inflow to the repository is contained in CCA Appendix MASS, Section MASS.7.***

~~There are at least three different alternative models that the DOE evaluated for explaining brine inflow. One conceptual model, the far-field flow model, is for flow from the far field in response to potentiometric gradients through naturally interconnected intergranular pore spaces. There is experimental evidence supporting this model in anhydrite interbeds and some non-anhydrite intervals. Experimental results from very pure halite are ambiguous with respect to this model: results can be interpreted either as very low permeability (near-complete absence of interconnected pore space); or as a lithology in which fluid is not responsive to applied pressure gradients. In the first case, potentiometric flow models can be used effectively with very low permeability values. In the second case, which would imply a conditional exception to the potentiometric flow model, a potentiometric model would not be appropriate for use.~~

~~Numerous parameters are necessary to describe flow in terms of potentiometric equations. These include properties describing the rock formation: porosity, permeability, density, rock compressibility; and properties describing fluid flow and fluid interactions: relative permeability, capillary pressure, fluid compressibility, fluid density, and fluid viscosity. Within the conceptual model, few limits are imposed on the spatial variability or functional dependence of these properties. It is known, for example, that the pore structure and composition of the Salado are not uniform, which leads to spatial heterogeneity in rock properties both by layering and within each layer. Fluid properties are known to be functions of pressure, temperature, chemical composition, and saturation.~~

~~A second conceptual model, the redistribution model, proposes that interconnected pore spaces do not exist naturally in most lithologic units in the Salado. Interconnected networks form as the result of fracturing and creep around excavations. Potentiometric flow occurs in interconnected networks, but because the interconnectedness is of limited extent, the volume of brine that can flow is severely limited compared to the naturally interconnected case. A numerical model based on the redistribution concept was developed and applied to the small-scale brine inflow (SSBI) data set (McTigue 1993). The redistribution-based model allowed the use of a more realistic capacitance for the formation response than do far-field flow models with far-field properties.~~

The third conceptual model for flow, the clay consolidation model, arises from observations made as part of the BSEP. On the basis of observations recorded during more than nine years of ~~underground observations (Deal and Case 1987; Deal and Roggenthen 1989; Deal et al. 1987, 1989, 1991a, 1991b, 1993), this model proposes that the most significant source of brine flowing into the repository is clay layers exposed by excavation. According to the model, (1) clay layers compact and yield brine when stresses are relieved near the excavation and (2) flow through other lithologic units is negligible.~~

~~Since definitive data do not exist to reconcile these three alternatives, the DOE has implemented the far-field flow model because it results in a range of variability in brine inflow that covers the other two alternative models.~~

The first principle in the conceptual model for fluid flow in the repository is that gas and brine can be both present and mobile (two-phase flow), governed by conservation of energy and mass and by Darcy's Law for their fluxes (see Appendix ~~BRAGFLO~~***PA***, Section ***PA-***4.***2***~~1 through 4.4~~). Consistent with typical concepts of two-phase flow, the phases can affect each other by

impeding flow caused by partial saturation (relative permeability effects) and by affecting pressure caused by capillary forces (capillary pressure effects).

The flow of brine and gas in the repository is assumed to behave as two-phase, immiscible, Darcy flow (see Appendix ***PA***~~BRAGFLO~~, Section ***PA-***4.***2***~~8 and 4.9~~). BRAGFLO is used to simulate brine and gas flow in the repository and to incorporate the effects of disposal room closure and gas generation. Fluid flow in the repository is affected by the following factors:

- the geometrical association of pillars, rooms, and drifts; panel closure caused by creep; and possible borehole locations;
- the varied properties of the waste areas resulting from creep closure and heterogeneous contents;
- flow interactions with other parts of the disposal system; and
- reactions that generate gas.

The geometry of the panel around the intrusion borehole is consistent with the assumption that fluid flow there will occur directly toward or directly away from the borehole. The geometry represents a semi-circular volume north of the borehole and a semi-circular volume south of the borehole (representing the assumption of radial flow in a subregion of a two-dimensional representation of the repository~~). Around the shaft, the assumption of convergent or divergent flow is made, and implemented with a similar gridding technique.~~

Approximating convergent and divergent flow around the intrusion borehole ~~and the shaft~~ creates ***a***~~two~~ narrow neck~~s~~ in the otherwise fairly uniform width grid in the region representing the repository. In the undisturbed performance scenario and under certain conditions in other scenarios, flow in the repository may pass laterally through th~~ese~~***is*** neck~~s~~. In reality, th***is***~~ese~~ neck~~s~~ do***es*** not exist. The~~ir~~ presence in the model is expected to have a negligible or conservative impact on model predictions compared to predictions that would result from use of a more realistic model geometry. The time scale involved and the permeability contrast between the repository and surrounding rock are sufficient that lateral flow that may occur in the repository is restricted by the rate at which liquid gets into or out of the repository, rather than the rate at which it flows through the repository.

Gas generation is affected by the quantity of liquid in contact with metal. However, the distribution of fluid in the repository can be only approximated. For example, capillary action can create wicking that would increase the overall region in which gas generation occurs, but this cannot be modeled at the necessary resolution to fundamentally stimulate processes without undesirable effects on the duration of the model simulations. Therefore, as a bounding measure for gas generation purposes, brine in the repository is distributed to an extent greater than actually estimated by the Darcy flow models used and values of parameters chosen.

Option D panel closures and the surrounding rocks are represented by a group of materials, which include:

1. ***SMC,***

2. a material representing the empty drift and explosion wall,

3. a material representing healed DRZ, and

4. Marker beds.

SMC and healed DRZ materials are assigned permeability values that are sampled independently from a distribution ranging from 2×10^{-21} to 1×10^{-17} m^2. This value range is considered reasonable because the shape of the Option D closure assumes a compressive state and concrete permeability range similar to the tighter end of the 1997 PAVT permeability. This range captures the uncertainty in the long-term performance of the Option D panel closure design.

~~Panel closures are represented with a permeability of 1×10^{-15} square meters, which is equivalent to the DRZ permeability. This value is considered reasonable as verified by an analysis, which is presented as Attachment 7-1 of this appendix.~~

Modeling of flow within the repository is based on homogenizing the room contents into relatively large computational volumes. The approach ignores heterogeneities in disposal room contents that may influence gas and brine behavior in the room by causing fluid flow among channels or preferential paths in the waste, bypassing entire regions. Isolated regions could exist for several reasons:

- they may be isolated by low-permeability regions of waste that serve as barriers,
- connectivity with the interbeds may occur only at particular locations within the repository, or
- the repository dip may promote preferential gas flow in the upper regions of the waste.

For the CCA, t~~The~~ adequacy of the ***repository homogeneity assumption***~~homogenization approach~~ was examined in screening analyses DR-1 (Webb 1995) and DR-6 (Vaughn et al. 1995a). ~~To address room heterogeneity, this~~ ***The analyses***~~analysis~~ used an additional parameter in BRAGFLO to specify the minimum active (mobile) brine flow saturation (pseudo-residual brine saturation). Above this saturation, the normal descriptions of two-phase flow apply (that is, either the Brooks and Corey or van Genuchten and Parker relative permeability models). Below this minimum, brine is immobile, although it is available for reaction and may still be consumed during gas-generation reactions. The assumption of a minimum saturation limit ***was***~~is~~ justified based on the presumed heterogeneity of the waste and the ~~fact that~~***slight dip in*** the repository~~ dips slightly~~. The minimum active brine saturation was treated as an uncertain parameter and sampled uniformly between values 0.1 and 0.8 during the analysis. This saturation limit was applied uniformly throughout the disposal room ~~in order~~ to bound the impact of heterogeneities on flow (Webb 1995; Vaughn et al. 1995a). Results of this analysis showed that releases to the accessible environment in the baseline case (homogenization) are consistently higher.

The experimental and operations regions ~~are~~***were*** represented in performance assessment ***(for the CCA)*** by a fixed porosity of 18.0 percent and a permeability of 10^{-11} ~~square meters~~ ***m^2***. ~~This~~ ***The***

combination of low porosity and high permeability ~~will~~ conservatively overestimate***d*** fluid flow through these regions and limit the capacity of these regions to store fluids, thus potentially overestimating releases to the environment. This conclusion ~~is~~***was*** based on a screening analysis (Vaughn et al. 1995b) that examined the importance of permeability varying with porosity in closure regions (waste disposal region, experimental region, and operations region). To perform this analysis, a model for estimating the change in permeability with porosity in the closure regions ~~(waste disposal region, experimental region and operations region)~~ was implemented in BRAGFLO. A series of BRAGFLO simulations was performed to determine whether permeability varying with porosity in ***the*** closure regions could enhance contaminant migration to the accessible environment. Two basic scenarios were considered in the screening analysis, undisturbed performance and disturbed performance. To assess the sensitivity of system performance on dynamic permeability in the closure regions, CCDFs of normalized contaminated brine releases were constructed and compared with the corresponding baseline conditional CCDFs. The baseline model treated permeabilities in the closure regions as fixed values. Results of this analysis showed that the inclusion of dynamic closure of the waste disposal region, experimental region, and operations region in BRAGFLO ***resulted***~~results~~ in computed releases to the accessible environment that are essentially equivalent to the baseline case.

A separate analysis (Park and Hansen 2003) examined the possible effects of heterogeneity in waste container and waste material strength on room closure. The analysis of room closure found that the room porosity may vary widely depending on the type of waste container and on the emplacement of waste in the repository. However, analysis of a separate PA (Hansen et al. 2003a) found that PA results are relatively insensitive to the uncertainty in room closure and room porosity. The conclusions of the separate PA are summarized in Section MASS-21.0.

MASS-7.1 Flow Interactions with the Creep Closure Model

The dynamic effect of halite creep and room consolidation on room porosity is modeled only in the waste disposal region. Other parts of the repository, such as the experimental region and the operations region, are modeled assuming fixed (invariant with time) properties. In these regions, the permeability is held at a fixed high value representative of unconsolidated material, while the porosity is maintained at relatively low values associated with highly consolidated material. It is assumed that this combination of low porosity and high permeability conservatively overestimates flow through these regions and minimizes the capacity of this material to store fluids, thus maximizing the release to the environment. To examine the acceptability of this assumption, a screening analysis (Vaughn et al. 1995c) evaluated the effect of including closure of the experimental region and operations region. In this analysis, consolidation of the experimental region and operations region was implemented in BRAGFLO by relating pressure and time to porosity using a porosity-surface method. The porosity surface for the experimental region and operations region differs from the one used for consolidation of the disposal room and is based on an empty excavation (see Appendix ***PA, Attachment*** PORSURF). Results of the screening analysis showed that disregarding dynamic closure of the experimental region is acceptable because it is conservative: lower releases occur when closure of the experimental region and operations region is computed compared to simulations with time-invariant high permeability and low porosity.

MASS-7.2 Flow Interactions with the Gas Generation Model

Gas generation affects repository pressure, which in turn is an important parameter in other processes such as two-phase flow, creep closure, and ~~interbed~~ fracturing ***of the interbeds and DRZ.*** Gas generation processes considered in performance assessment calculations include anoxic corrosion and microbial degradation. Radiolysis is excluded from performance assessment calculations on the basis of laboratory experiments and a screening analysis (Vaughn et al. 1995d) that concluded that radiolysis does not significantly affect repository performance.

In modeling gas generation, the effective liquid in a computational cell is the computed liquid in that cell plus an adjustment to account for the uncertainty associated with wicking by the waste (see Appendix ***PA***~~BRAGFLO~~, Section ~~7.2.9~~***PA-4.2***). Capillary action (wicking) is the ability of a material to carry a fluid by capillary forces above the level it would normally seek in response to gravity. Because the current gas-generation model computes substantially different gas-generation rates depending on whether the waste is wet or merely surrounded by water vapor, the physical extent of wetting could be important. A screening analysis (Vaughn et al. 1995e) examined wicking and concluded that it should be included in performance assessment calculations. The baseline gas-generation model in BRAGFLO accounts for corrosion of iron and microbial degradation of cellulosics. The net reaction rate of these processes depends directly on brine saturation: an increase in brine saturation will increase the net reaction rate by weighting the inundated portion more heavily and the slower humid portion less heavily. To simulate the effect of wicking on the net reaction rate, an effective brine saturation, which includes a wicking saturation contribution, is used to calculate reaction rates rather than the actual brine saturation. To account for uncertainty in the wicking saturation contribution, this contribution was sampled from a uniform distribution that ranged from 0.0 to 1.0 for each BRAGFLO simulation in the analysis.

MASS-8.*0* GAS GENERATION

This model represents the possible generation of gas in the repository by corrosion of steel and microbial degradation of cellulosic, plastic, and rubber ***(CPR) materials***. Additional discussion of this topic may be found in ~~Appendices WCA (Section WCA.5.1), BRAGFLO (Section 4.13), SOTERM (Section SOTERM.2.2), and SCR (Section SCR.2.5.1).~~ ***Appendix PA, Section PA-4.2.5 and Attachment SCR (FEPs W44 through W48, W53, and N71) and Section 6.4.3.3.***

Gas will be produced in the repository by a variety of chemical reactions, principally those between brine, metals, microbes, ~~cellulosics, plastics, and rubber materials~~ ***CPR materials*** and by liberation of dissolved gases to the gaseous phase. The processes assumed for long-term performance are anoxic corrosion of steel waste containers and ***Fe-base*** metals in the waste and ***possible*** microbial ~~degradation~~***consumption*** of ***CPR materials*** ~~perhaps, plastics and rubbers~~ in the waste ***(a significant quantity of plastic is also present as drum liners).*** Anoxic-corrosion reactions between brine and steel are expected to occur and produce H_2; they are included in the conceptual model. Microbial ~~degradation~~***consumption*** of cellulosics ~~and perhaps~~, plastics and rubbers, might occur. If it does, it may produce various gases, primarily CH_4 and CO_2. However, by reaction with the MgO backfill that will be emplaced to control the chemistry of the repository, CO_2 produced by microbial ~~degradation~~***activity*** will be rapidly removed from the

gaseous phase (see Appendix ***PA, Attachment*** SOTERM, Section SOTERM-2.2.2***;*** and ~~Chapter 6.0,~~ Section 6.4.3.4). Other gases such as N_2 and H_2S produced by microbial ~~degradation~~***activity*** are insignificant in quantity (see ***CCA Appendix MASS,*** Attachment 8-1). Thus the conceptual model for gas generation ~~is~~ ***assumes*** that anoxic corrosion of steel will produce H_2; microbial ~~degradation~~***consumption*** of ~~cellulosics, plastics, and rubber materials~~ ***CPR materials*** might occur and ~~might~~ produce ***CH_4, CO_2, and*** other gases, but any CO_2 produced ~~is~~***will be*** rapidly removed by reaction with MgO ~~backfill~~.

In the conceptual model, the rate of gas production in the repository by anoxic corrosion can be limited by several factors. Anoxic corrosion cannot occur unless brine (water) is present and in contact with steel. The corrosion rate is assumed to be dependent on brine saturation. Because anoxic corrosion consumes steel, the rate of gas production can be limited by the quantity of steel left in the repository. Because corrosion is a surface reaction, it proceeds at quantifiable rates per unit surface area of steel. In addition, anoxic corrosion consumes water. Because of these factors, the rate of gas generation in the repository can vary through time as conditions change. It is assumed that anoxic corrosion can occur in the repository as soon as the shafts are sealed.

Microbial ~~degradation~~***consumption*** of ~~cellulosics, plastics, and rubbers~~***CPR materials*** is limited by several factors, chiefly the long-term viability of microbes in the repository. Whether microbes ~~degrade~~***consume*** plastics and rubbers is also important. The rate of microbial ~~degradation~~***production*** is dependent on brine saturation. Because of uncertainty, however, it is assumed that there is no effect of microbial ~~degradation~~***activity*** on brine (water) content in the repository.

A limited quantity of O_2 will be trapped in the panels after repository closure. However, this O_2 will be consumed quickly by both oxic corrosion and ***aerobic*** microbial ~~degradation~~***activity***, and ~~the~~ reducing ~~environment~~***conditions*** will ~~be~~ domina~~nt~~***te*** in the repository over 10,000 years. The contribution of oxic corrosion and ~~biodegradation~~***aerobic microbial activity*** to overall gas production is negligible. Thus, oxic reactions are not considered in the conceptual model for gas generation.

Addition of an MgO ~~backfill~~***engineered barrier*** significantly reduces the impact of microbial ~~dgeneration~~***production*** of CO_2 ***(see Appendix PA, Attachment SOTERM)***~~(see Attachment 8-2)~~. As discussed in Section 6.4.3.4, the MgO backfill will react with carbon dioxide produced by microbial degradation and remove it from the gaseous phase.

Because the conceptual model ~~discusses~~***comprises*** the general processes and interactions assumed to occur without direct reference to the mathematical equations used, no parameters are defined by this conceptual model. The mathematical model used to implement it, the average-stoichiometry model, is discussed in Section 6.4.3.3~~ and Attachment 8-2~~. The most important parameter in the average-stoichiometry model is the rate at which gas ~~generation~~ ***production*** occurs with brine and steel present, because this is the principal control on the total quantity of gas generated. The assumptions made about the principal reactions and their stoichiometr~~y~~***ies*** are also important, however, because they affect the quantity of gas created per unit quantity of steel and water reacted.

The feedback between the gas generation conceptual model and the repository fluid flow conceptual model is important to understand. Gas ~~generation~~***production*** cannot continue for long with the low initial quantity of liquid present in the waste, as specified by waste-acceptance criteria. For gas ~~generation~~ ***production*** to occur, brine must flow into the repository; for gas ~~generation~~ ***production*** to be sustained, brine consumed by gas ~~generation~~ ***production*** must be replenished. Gas ~~generation~~ ***production***, however, tends to increase repository pressure and keep brine from flowing into it. Thus the rates at which various processes proceed are important in determining the conditions of the repository. There is important feedback as well between the gas-generation model and other conceptual models through pressure effects, such as those calculating creep closure (Section 6.4.3.1), interbed fracturing (Section 6.4.5.2), two-phase flow (Section 6.4.3.2), and the radionuclide release associated with spalling and direct brine release during an inadvertent drilling intrusion (Section 6.4.7).

Single-process laboratory studies of anoxic corrosion of steels and Al-based materials by R. E. Westerman and his colleagues at Pacific Northwest ***National*** Laboratory (PN***N***L) from November 1989 through September 1995 have shown that the factor with the greatest effect on the rate of H_2 generation by anoxic corrosion is the quantity of brine in WIPP disposal rooms (***see also CCA Appendix MASS,*** Attachment 8-2). This is because anoxic corrosion occurs rapidly under inundated conditions, but not at all under humid conditions. The pressure difference between WIPP disposal rooms and the far field and the porosity of the room contents also affect the extent of brine inflow and outflow and, hence, the anoxic-corrosion rate. Because the average-stoichiometry model is incorporated in BRAGFLO, gas ~~generation~~ ***production*** is coupled with brine and gas inflow and outflow. Moreover, because BRAGFLO uses a porosity surface to simulate room closure (Butcher and Mendenhall 1993), it also couples gas ~~generation~~ ***production*** to room closure. Telander and Westerman (1993***, 1997***) and subsequent studies of anoxic corrosion at PN***N***L have shown that pH, pressure, and the composition of the gaseous phase also affect the H_2 ~~generation~~ ***production*** rate.

The greatest uncertainty in modeling gas generation in WIPP disposal rooms is whether microbial gas generation will occur and, if so, to what extent it will occur and what its effects will be. The following sources of microbial uncertainty have been described:

- whether microorganisms capable of carrying out the potentially significant respiratory pathways identified by Brush (1990) (denitrification ***sulfate (***SO_4^{2-}***)*** reduction, and methanogenesis) will be present when the repository is filled and sealed,
- whether these microbes will survive for a significant fraction of the 10,000-year period of performance of the repository,
- whether sufficient H_2O will be present in the waste or brine,
- whether sufficient electron acceptors (oxidants) will be present and available,
- whether enough nutrients, especially N and P, will be present and available,
- whether microbes will consume significant quantities of plastics and rubbers during the 10,000-year period of performance of the repository, and

- the stoichiometry of the overall reaction for each significant respiratory pathway, especially the number of moles of electron acceptors, nutrients, gases, and H_2O consumed or produced per mole of substrate consumed.

With regard to the first five of these uncertainties, it has been concluded that, although significant microbial gas production is possible, it is by no means certain. ~~Therefore, it has been estimated that significant microbial gas generation in WIPP disposal rooms will occur half of the time; and in half of the cases that significant microbial degradation occurs, microbes will consume all of the plastics and rubbers in the repository after they consume all of the cellulosics~~. ***To incorporate this uncertainty in PA, it is assumed that there is a probability of 0.50 for significant microbial activity. In the event of significant microbial activity, microbes would consume 100 percent of the cellulosics in the repository. Furthermore, there is a probability of 0.50 that microbes would consume all of the plastics and rubbers after consuming all of the cellulosics. Thus, there is microbial consumption of all of the cellulosics, but no plastics or rubbers, in about 25 percent of the PA realizations (vectors); microbial consumption of all of the CPR materials in 25 percent of the vectors; and no microbial activity at all in the remaining 50 percent of the vectors*** (***see CCA Appendix MASS,*** Attachment 8-3).

Single-process laboratory studies of microbial consumption of cellulosics by A.J. Francis and his colleagues at Brookhaven National Laboratory from May 1991 through September ~~1995~~***2003*** showed that if significant microbial activity occurs, the factor with the greatest effect on the microbial gas-generation rate is the quantity of brine in the repository (see Francis and Gillow 1994***, 2000; Francis et al. 1997; Gillow and Francis 2001a, 2001b, 2002a, 2002b; CCA Appendix MASS,*** Attachment 8-2). This is because microbial gas ~~generation~~ ***production*** occurs rapidly under inundated conditions, but at much lower rates under humid conditions. ~~Francis and Gillow (1994)~~ ***These studies*** also found that inoculation with halophilic microbes from the WIPP site and nearby lakes, amendment with NO_3^- (an electron acceptor), amendment with nutrients, and addition of bentonite (a previously proposed backfill material) affect the rate or extent of microbial gas generation. Other factors that could affect the rate or extent of microbial gas generation, but which ~~Francis and Gillow (1994)~~ ***these studies*** did not quantify, are the pH; the dissolved or suspended concentrations of actinides or other heavy metals, which could inhibit or preclude microbial activity; and the concentrations of microbial byproducts, which could inhibit or preclude additional microbial activity. High pressure will not preclude or even inhibit microbial activity significantly, even when it increases to 150 atmospheres (lithostatic pressure at the depth of the repository).

Data summarized by Molecke (1979) imply that radiolysis of ~~cellulosics, plastics, and rubbers~~ ***CPR materials*** will not be a significant, long-term gas-generation process in WIPP disposal rooms. (Radiolysis here refers to α radiolysis, the breaking of chemical bonds by α particles emitted during the radioactive decay of the actinide elements in TRU waste. Because molecular dissociation caused by other types of radiation will be insignificant in a TRU-waste repository such as the WIPP, this discussion considers only α radiolysis.) Based on calculations using the results of laboratory studies of brine radiolysis carried out for the WIPP by Reed et al. (1993) on estimates of the quantities of brine that could be present in the repository after filling and sealing, and on estimates of the solubilities of Pu, Am, Np, Th, and U summarized by Trauth et al. (1992), it was concluded that radiolysis of H_2O will not significantly affect the

overall gas or H_2O content of the repository (see Appendix ***PA, Attachment*** SCR***, FEP W52,*** ~~Section SCR.2.5.1.3.1~~).

Gas generation models are implemented in BRAGFLO with the assumption that the substrates (CPR materials and Fe-base metals) are homogeneously distributed throughout the waste. A separate PA (Hansen et al. 2003a) examined the possible effects of heterogeneity in substrate concentrations on PA results, and found that PA results are insensitive to the heterogeneity in substrate concentrations. The conclusions of the separate PA are summarized in Section MASS-21.0.

MASS-8.1 Historical Context of Gas Generation Modeling

See CCA Appendix MASS, Section MASS.8.1 for historical information that led to the CCA gas generation conceptual model. ~~The DOE performed laboratory studies of gas generation during the late 1970s to support the development of TRU waste acceptance criteria (Molecke 1978, 1979; Sandia National Laboratories 1979). For the most part, these laboratory studies comprised single-process experiments (one gas-generation process studied at a time) on microbial activity and radiolysis with nonradioactive and some radioactive simulated TRU waste. There was very little work on anoxic corrosion. Based on laboratory measurements on samples obtained by drilling from the surface, the permeability of the Salado appeared to be high enough for rapid migration of gas from the repository, even given the highest gas-generation rates summarized by Molecke (1979). Therefore, the DOE concluded that further studies of gas generation were unnecessary.~~

~~In 1987, preliminary performance assessment calculations on the effects of human intrusion identified inflow of intergranular Salado brine as a concern for the long-term performance of the repository. In early 1988, the DOE began to examine the possible effects of processes such as anoxic corrosion of steels and microbial degradation of cellulosics on the H_2O content of WIPP disposal rooms. Brush and Anderson (1989a) concluded that these processes could affect the H_2O content as significantly as brine inflow. Furthermore, they concluded that these processes could also produce significant quantities of gas. Meanwhile, in situ measurements in the WIPP underground workings revealed that the permeability of the Salado was much lower than believed in the late 1970s.~~

~~Systems analysis carried out by Lappin et al. (1989) to support the 1990 Supplemental Environmental Impact Statement, which used gas-generation assumptions from Brush and Anderson (1989a, 1989b, and 1989c), the rates-and-potentials gas-production model of Lappin et al. (1989), and new in situ permeabilities, demonstrated that gas would affect the overall performance of the repository if present in significant quantities.~~

~~Therefore, the DOE initiated laboratory studies of gas generation in February 1989. These studies have comprised mainly single-process experiments on anoxic corrosion, microbial activity, and radiolysis, mostly with nonradioactive, simulated CH-TRU waste (Brush 1990; Brush et al. 1991a, 1991b, 1993; Reed et al. 1993; Telander and Westerman 1993; Francis and Gillow 1994).~~

~~The DOE has also developed two additional gas-generation models since 1989. The WIPP Performance Assessment Division (1991) developed the average stoichiometry gas-generation model and incorporated it into BRAGFLO, which also simulates room closure. Incorporation of the average stoichiometry model into BRAGFLO thus coupled this gas-generation model with the hydrologic and geomechanical models used for performance assessment. The WIPP Performance Assessment Division (1991) and Brush et al. (1994) developed the average stoichiometry and the reaction-path gas-generation models, respectively, based on the results of the single-process laboratory studies that were restarted in 1989. However, although these laboratory studies considered only one gas-generation process at a time (anoxic corrosion, microbial activity, or radiolysis), they did, at least to some extent, simulate some of the possible interactions between these processes. For example, the study of anoxic corrosion by Telander and Westerman (1993) considered the effects of the microbially produced gases CO_2 and H_2S on corrosion, and Brush et al. (1994) included passivation of steels and other Fe-based metals by CO_2 and H_2S in the reaction-path model.~~

~~Work began on the reaction-path gas-generation model in 1992, which includes more gas-generation processes than the average stoichiometry model and the interactions among these processes (Brush et al. 1994). It was recommended to replace the average stoichiometry model in BRAGFLO with the reaction-path model. However, in November 1995, the DOE decided to terminate all work on the reaction-path model and to continue to use the average stoichiometry model in BRAGFLO. The rationale for the decision is documented in Attachment 8-1. The main advantage of the reaction-path model relative to the average stoichiometry model is that the former includes passivation of steels by microbially produced CO_2 and H_2S. However, the results from laboratory studies of anoxic steel corrosion fail to support passivation of steels by CO_2. Therefore, the main advantage of the reaction-path model no longer exists. In addition, the experimental results show that anoxic steel corrosion does not stop at about 70 atm hydrogen pressure as predicted by the reaction-path model. Because of these reasons, the reaction-path model is not used in BRAGFLO calculations.~~

MASS-9.*0* CHEMICAL CONDITIONS

~~Topics in the~~***The*** models used for chemical conditions in the repository are discussed in ***Appendix BARRIERS and*** Appendix ***PA, Attachment*** SOTERM and ~~Chapter 6.0 (~~Section 6.4.3.4).

MASS-10.*0* DISSOLVED ACTINIDE SOURCE TERM

~~Topics in the~~***The*** models used for the dissolved actinide source term in the repository are discussed in Appendix ***PA, Attachments*** SOTERM ***and SCR and*** ~~Chapter 6.0~~ Section 6.4.3.5) ~~and Appendix SCR (Sections SCR.2.5.2 and SCR.2.5.3).~~

MASS-11.*0* COLLOIDAL ACTINIDE SOURCE TERM

~~Topics in the~~***The*** models used for the colloidal actinide source term are discussed in Appendix ***PA, Attachment*** SOTERM (Section SOTERM.6) and ~~Chapter 6.0 (~~Section 6.4.3.6~~)~~.

MASS-12.*0* SHAFTS AND SHAFT SEALS

The conceptual model for the shafts and shaft seals used in the performance assessment has been chosen to provide a reasonable and realistic basis for simulating long-term fluid flow through the shaft seal system and to allow evaluation of the effect that uncertainty about the long-term properties of the shaft seal system may have on cumulative radionuclide releases from the disposal system. The conceptual model ***and seal system design are***~~is~~ also discussed in ~~Chapter 6.0 (~~Section 6.4.4~~)~~ and ***CCA*** Appendix SEAL (Section 2).

The conceptual model of the seals is based on results of detailed numerical models of the shaft seal system design. These models were developed to evaluate the performance of the shaft seal system under a range of conditions. Both fluid flow and structural response of the system have been evaluated. The principal uncertainties associated with the detailed models follow:

- reconsolidation of the crushed salt component,
- construction, permeability, and gas threshold pressure of the clay components, and
- damage, permeability, healing, and character of the Salado ~~and Rustler~~ disturbed rock zones.

These uncertainties are also present in the performance assessment model and have been accounted for in the values specified for seal parameters. The consequences of uncertainty in seal component performance were a primary motivation in the development of the proposed seal system design. Although there is uncertainty in many of the materials and models, the shaft will be completely filled with high density, low permeability materials. The use of multiple materials and components for each sealing function results in a robust system. Time dependency of the performance of seal components is incorporated directly into the model through temporal variation in seal properties.

The processes that can affect the performance of the shaft seals—structural, hydraulic, and coupled structural and hydrological—are discussed in some detail in ***CCA*** Appendix SEAL***,*** ~~(~~Sections 7 and 8~~)~~. Evaluation of these issues required the use of existing structural and both single-and two-phase flow codes. In addition, development of conceptual and numerical models for crushed salt reconsolidation, the disturbed rock zone, and the shaft seal system was required. These models have been reviewed by independent, qualified experts, are well documented, and have been developed within an accepted quality assurance program. Codes used in the analyses include SPECTROM-32 (structural) (Callahan 1994), SWIFT II (single-phase flow) (Reeves et al. 1986), and TOUGH2 (multi-phase flow) (Pruess 1991). These codes were selected for their capability to simulate the processes thought to affect seal performance. They are also well-documented, accepted, and widely used within the scientific community. The codes were modified to implement the conceptual models specific to the seals, and these modifications were made within a program that establishes criteria for assuring software quality.

The BRAGFLO model of the ***shaft*** seal system requires consistency with parameters associated with the surrounding system. ***The BRAGFLO shaft seal model implemented for the 2004 PA calculations grouped several shaft seal materials into two composite materials having properties derived from the combination of grouped materials in series. For example, the***

permeability of the material used to represent the lower portion of the shaft seal that lies in the Salado formation is derived from the permeability and thickness of the asphalt, concrete crushed salt, and clay layers of the seal in this horizon. This permeability changes after 200 years to incorporate the combined effects of the consolidation of these materials. The effects of the halite DRZ surrounding the shafts is included in the derivation of the composite properties used in the BRAGFLO model. A detailed description of the shaft model used in the 2004 PA BRAGFLO calculations can be found in James and Stein (2002 and 2003). ~~For example, the permeability of the crushed salt component should always be greater than or equal to that of the intact halite. Similarly, the calculation of the effective halite DRZ permeability requires the permeability of intact halite as input. As discussed in Appendix SEAL (Section 1.4), procedures in performance assessment have been implemented to ensure these parameter consistency concerns are met.~~

MASS-12.1 Historical Development of the Shaft Seals

The four shafts into the repository will be sealed after completion of disposal activities at the WIPP. The shaft seal system design has evolved over time (Stormont 1988; Nowak et al. 1990; DOE 1995). The Initial Reference Seal System Design proposed a two-component design to achieve a sealing strategy with two phases: concrete and clay seals formed a short-term seal, and a crushed salt seal formed long-term protection. The use of native rock (that is, crushed salt) as a permanent sealing material is considered the most effective means to eliminate the shafts as a preferred pathway for migration of hazardous constituents. Because some interim period must pass for the crushed salt to reconsolidate to sufficiently high densities, short-term seals were proposed as a means to prevent fluid migration during the interim. Estimates of this interim period ranged from 100 to 200 years.

Seal design changes and refinements have been incorporated into the conceptual model of the seals used by the DOE (Bertram-Howery et al. 1990; WIPP Performance Assessment Department 1991; Sandia WIPP Project 1992). Performance assessments conducted prior to 1992 addressed general sealing issues but did not include specific seal components.

Results of the scoping calculations using the DCCA model demonstrated that low-permeability materials were required for the shaft seals (DOE 1995, Appendix D). However, the simplicity of the conceptual model limited the applicability of results to the detailed seal system design.

The shaft seal design for the WIPP is presented in ***CCA*** Appendix SEAL (Sections 4 and 5).

MASS-13.*0* SALADO

The purpose of this model is to reasonably represent the effects of fluid flow in the Salado on long-term performance of the disposal system. The conceptual model is also discussed in Section 6.4.5.

Fluid flow in the Salado is considered in the conceptual model of long-term disposal system performance for several reasons. First, some liquid could move from the Salado to the repository because of the considerable gradients that can form for liquid flow inward to the repository. This possibility is important because such fluid can interact with creep closure, gas generation,

actinide solubility~~y~~***ies***, and other processes occurring in the repository. Second, gas generated in the repository is thought to be capable of fracturing the Salado interbeds under certain conditions, creating increased permeability channels that could be pathways for lateral transport. The pathway of lateral transport in intact Salado is also modeled, but it is considered unlikely to result in any significant radionuclide transport to the accessible environment boundary.

The fundamental principle in the conceptual model for fluid flow in the Salado is that it is a porous medium within which gas and brine can be both present and mobile (two-phase flow), governed by conservation of energy and mass, and by Darcy's Law for their fluxes (see Appendix ~~BRAGFLO~~***PA***, Sections ***PA-***4.***2***~~1 through 4.4~~). Consistent with typical concepts of two-phase flow, each phase can affect the other by impeding flow because of partial saturation (relative permeability effects) and by affecting pressure by capillary forces (capillary pressure effects). It is assumed that no waste-generated gas is present initially***. Future states are modeled as producing gas by corrosion and microbial activities. Should high pressure develop over the regulatory period, it is allowed to access marker beds in the Salado.***~~, but gas can enter the interbeds. It is expected that the low permeability of impure and pure halite intervals of the Salado will prevent gas from penetrating because of the expected high capillary pressure for these units.~~

Some variability in composition exists between different horizons of the Salado. The largest differences occur between the anhydrite-rich layers called interbeds and those dominated by halite. Within horizons dominated by halite, composition varies from nearly pure halite to halite plus several percent other minerals, in some instances including clay (see Chapter 2.0, Section 2.1.3.4). The Salado is modeled as impure halite except for those interbeds that intersect the DRZ near the repository. This conceptual model and an alternative model that explicitly represented all stratigraphically distinct layers of the Salado near the repository (Christian-Frear and Webb 1996) produced similar results.

From other modeling and theoretical considerations, flow between the Salado and the repository is expected to occur primarily through interbeds that intersect the DRZ. Because of the large surface areas between the interbeds and surrounding halite, the interbeds serve as conduits for the flow of brine in two directions: from halite to interbeds to the repository, or, for brine flowing out of the repository, from the repository into interbeds and then into halite. Because the repository is modeled as a relatively porous and permeable region, brine is considered most likely (but not constrained) to leave the repository through MB139 below the repository because of the effect of gravity. ***If repository pressures become sufficiently high, gas is modeled to exit the repository via the marker beds in the proximity of the disposal room.*** ~~Gas is considered most likely (but not constrained) to leave the repository through anhydrite interbeds above the repository.~~

The effect of gravity may also be important in the Salado because of the slight and variable natural stratigraphic dip. For long-term performance modeling, the dip in the Salado within the domain is taken to be constant and 1 degree from the north to south.

Fluid flow in the Salado is conceptualized as occurring either convergently upon the repository, or divergently from it, as discussed in detail in Section 6.4.2.1. Because the repository is not conceptualized as homogeneous, implementing a geometry for the conceptual model of

convergent or divergent flow in the Salado is somewhat complicated and is discussed in Section 6.4.2.1.

The conceptual model for Salado fluid flow has primary interactions with three other conceptual models. The interbed fracture conceptual model allows porosity and permeability of the interbeds to increase as a function of pressure. The repository fluid flow model is directly coupled to the Salado fluid flow model by the governing equations of flow in BRAGFLO (in the governing equations of the mathematical model, they cannot be distinguished), and it differs only in the region modeled and the parameters assigned to materials. The Salado model for actinide transport is directly coupled to the conceptual model for flow in the Salado through the process of advection.

MASS-13.1 High Threshold Pressure for Halite-Rich Salado Rock Units

A parameter used to describe the effects of two-phase flow is threshold pressure. The threshold pressure is important because it helps determine the ease with which gas can enter a liquid-saturated rock unit. For a brine-saturated rock, the threshold pressure is defined as "equal to the capillary pressure at which the relative permeability to the gas phase begins to rise from its zero value, corresponding to the incipient development of interconnected gas flow paths through the pore network" (Davies 1991, ***p.*** 9).

The threshold pressure, as well as other parameters used to describe two-phase characteristics, has not been measured for halite-rich rocks of the Salado. The Salado, however, is thought to be similar in pore structure to rocks for which threshold pressures have been measured (Davies 1991). Based on this observation, Davies (1991) postulated that the threshold pressure of the halite-rich rocks in the Salado could be estimated if an empirical correlation exists between rocks postulated to have similar pore structure.

Davies developed a correlation between threshold pressure and intrinsic permeability applicable to the Salado halites. (A similar correlation was developed for Salado anhydrites; subsequent testing confirmed that the correlation predicted threshold pressures accurately.) The correlation developed by Davies predicts threshold pressures in intact Salado halites on the order of 20 megapascals or greater (Davies 1991). This threshold pressure predicted by correlation is so high that for all practical and predictive purposes, no gas will flow into intact Salado halites (see Section 6.4.5.1).

Because threshold pressure helps control the flow of gas, and because the greatest volume of rock in the Salado is rich in halite, a high threshold pressure effectively limits the volume of gas that can be accommodated in the pore spaces of the host formation. Thus high threshold pressure is considered conservative as well as realistic, because if gas could flow into the pore spaces of Salado halite, repository pressures could be reduced dramatically.

MASS-13.2 Historical Context of the Salado Conceptual Model

See CRA Appendix MASS, Section MASS.13.2 for the historical information relating to the CCA Salado conceptual model. The Salado conceptual model is unchanged for CRA-2004.

~~In the 1980 FEIS (documented in Lappin et al. 1989, Table 1-1, 1-7 to 1-8), the Salado was assumed to be a confining bed, containing no circulating groundwater (Lappin et al. 1989, 7--87). Brine was thought to be present only in fluid inclusions and hydrous minerals and was assumed not to be present along grain boundaries. Gas permeability was estimated to be adequate to dissipate the volumes of gas potentially generated by the waste. There was no explicit recognition of any differing hydrologic role for the nonhalite interbeds.~~

~~Based on the results of early in situ permeability testing, the conceptual model of the Salado had changed by the time of publication of Lappin et al. (1989, Table 1-1, 1-7 to 1-8). Grain boundary brines were known to be present and were distinct compositionally from fluid inclusions. The Salado was interpreted to be brine saturated. The major contribution to fluid flow was interpreted to be movement of grain-boundary fluids, as a result of pore pressure gradients resulting from excavation. Darcy flow, assuming atmospheric boundary conditions within the repository (which was all that could be modeled at the time), probably over-predicted brine inflow. Far-field permeability (not distinguished between halites and anhydrites) was thought to be less than 10^{-21} to 10^{-22} square meters and possibly even effectively zero in undisturbed regions. Because gas would have to displace brines in the Salado, dissipation of significant volumes of gas would be difficult. The combination of gas-generation rates and low permeability would have led to pressures exceeding lithostatic unless these pressures were relieved: numerical models for altered anhydrites did not exist at that time. Except at seal locations, MB139 was thought to be a relatively high-permeability flow path directly under the excavations because of the development of open excavation-related fractures.~~

~~In the preliminary performance assessment completed in December 1992 (WIPP Performance Assessment Department 1992, 2-41 to 2-45), anhydrite interbeds provided the dominant pathway for fluid migration because of their relatively high permeability. New test data indicated permeabilities of 10^{-16} to 10^{-21} square meters for anhydrites and 10^{-20} to 10^{-24} square meters for halite. (The DOE interpreted the low ends of these ranges to be far-field permeabilities and the higher ends to results from excavation effects; see Sandia WIPP Project 1992, 2-56 to 2-57). It was newly recognized that there would be coupling between fluid flow, creep closure, and brine-dependent gas generation. No altered-anhydrite model was implemented in this preliminary performance assessment.~~

~~In 1994, the DOE concluded that the regional 1-degree stratigraphic dip could have an effect on fluid flow into and out of the repository. An altered-anhydrite model for interbed fracture under elevated gas pressures was implemented. Flow simulations incorporating detailed stratigraphy confirmed that simplifications considering only a lumped impure halite were adequate (Christian-Frear and Webb 1996). The potential for preferential brine outflow caused by channeling, fingering, updip flow, or fracturing was also recognized. Concern about the adequacy of the two-dimensional modeling simplification to provide reasonable estimates of three-dimensional brine inflow and outflow was thought to be potentially important, because of the addition of both dip and altered-anhydrite fracturing models. These concerns led to a number of modeling and analysis efforts to investigate the adequacy of performance assessment assumptions.~~

~~In 1995 and 1996, final analyses of the Room Q experiments showed experimental results to be consistent with a Darcy flow model.~~

MASS-13.3 The ~~Anhydrite Interbed~~ Fracture Model

The purpose of this model is to alter the porosity and permeability of the anhydrite interbeds ***and the DRZ*** if their pressure approaches lithostatic, simulating some of the hydraulic effects of fractures with the intent that unrealistically high pressures (~~much~~ in excess of lithostatic) do not occur in the repository or disposal system. The conceptual model is also discussed in Section 6.4.5.2.

In the 1992 preliminary performance assessment, repository pressures were shown to greatly exceed lithostatic pressure if a large quantity of gas was generated. Pressures within the waste repository and surrounding regions were predicted to be roughly 20 to 25 megapascals. It was expected that fracturing within the anhydrite marker beds would occur at pressures slightly below lithostatic pressure. An expert panel on fractures was convened to develop the conceptual bases for the fracturing within the anhydrite marker beds.

The porosity and permeability increases are conceptualized as occurring vertically throughout the affected interbed; in other words, throughout the porous medium as a whole rather than on discrete portions. This simplification facilitates numerical implementation and execution.

Two parametric behaviors must be quantified in the conceptual model. First, the change of porosity with pressure in the anhydrite marker beds must be specified. This is done with a relatively simple equation, described in Appendix ***PA***~~BRAGFLO (~~***,*** Section ***PA-***4.***2***~~10)~~, that relates porosity change to pressure change using an assumption that the fracturing can be thought of as increasing the compressibility of interbeds. Parameters in the model are treated as fitting parameters and have little relation to physical behavior except that they affect the porosity change. The second parametric behavior is the change of permeability with pressure, which is incorporated by a functional dependence on the porosity change. It is assumed that a power function is appropriate for relating the magnitude of permeability increase to the magnitude of porosity increase. The parameter in this power function, an exponent, is also treated as a fitting parameter and can be set so that the behavior of permeability increase with porosity increase fits the desired behavior.

The fracture enhancement model assumes fracture propagation is uniform in the lateral direction to flow within the marker beds in the absence of dip. The 1-degree dip modeled in BRAGFLO may affect fracture propagation direction. That is, within the accuracy of the finite difference grid, a fracture will develop radially outward. This would not account for fracture fingering or a preferential fracturing direction; however, no existing evidence supports heterogeneous anhydrite properties that would contribute to preferential fracture propagation. This evidence is discussed in ***CCA Appendix MASS,*** Attachment 13-2***)***.

The maximum enhanced fracture porosity controls the storativity within the fracture. The extent of the migration of the gas front into the marker bed is sensitive to this storativity. The additional storativity caused by porosity enhancement will mitigate gas migration within the marker bed. The enhancement of permeability by marker-bed fracturing will make the gas more mobile and will contribute to longer gas-migration distances. Thus the effects of porosity enhancement at least partially counteract the effects of permeability enhancement in affecting the gas-migration distances.

Because intact anhydrite is partially fractured, the pressure at which porosity or permeability changes are initiated is close to the initial pressure within the anhydrite. The fracture treatment within the marker beds will not contribute to early brine drainage from the marker bed, because the pressures at these times are below the fracture initiation pressure.

The input data to the interbed fracture model (see Appendix ***PA, Attachment*** PAR~~, Table PAR-36~~) were chosen deterministically to produce the appropriate pressure and porosity response as predicted by a linear elastic fracture mechanics (LEFM) model, as discussed in Mendenhall and Gerstle (1993).~~ Results from this performance assessment show that repository pressures do not exceed the full fracture pressure of approximately 16.5 megapascals, a value slightly higher than lithostatic pressure.~~

MASS-13.4 Flow in the Disturbed Rock Zone

The conceptual model for the DRZ around the waste disposal, operations, and experimental regions has been chosen to provide a reasonably conservative estimate of fluid flow between the repository and the intact halite and anhydrite marker beds. The conceptual model is also discussed in Section 6.4.5.3 of this application.

The conceptual model implemented in the performance assessment uses values for the permeability and porosity of the DRZ that do not vary with time. A screening analysis examined an alternative conceptual model for the DRZ in which permeability and porosity changed dynamically in response to changes in pressure (Vaughn et al. 1995). This analysis implemented a fracturing model in BRAGFLO for the DRZ. This fracturing model is identical to the existing anhydrite interbed alteration model. In this model, formation permeability and porosity depend on brine pressure as described by Freeze et al. (1995, 2-16 to 2-19) and Appendix ***PA,*** ~~BRAGFLO (~~Section ***PA-***4.***2.***1~~0)~~. This model permits the representation of two important formation alteration effects. First, pressure build-up caused by gas generation and creep closure within the waste will slightly increase porosity within the DRZ and offer additional fluid storage with lower pressures. Second, the accompanying increase in formation permeability will enhance fluid flow away from the DRZ. Because an increase in porosity tends to reduce outflow into the far field, parameter values for this analysis were selected so that the DRZ alteration model greatly increases permeability while only modestly increasing porosity.

Two basic scenarios were considered in the screening analysis by Vaughn et al. (1995), undisturbed performance and disturbed performance. Both scenarios included a 1-degree formation dip downward to the south. Intrusion event E1 is considered in the disturbed scenario and consists of a borehole that penetrates the repository and pressurized brine in the underlying Castile. Two variations of intrusion event E1 were examined, E1 updip and E1 downdip. In the E1 updip event, the intruded panel region was located on the updip (north) end of the waste disposal region, whereas in the E1 downdip event, the intruded panel region is located on the downdip (south) end of the disposal region. These two different geometries permitted evaluation of the possibility of increased brine flow into the panel region caused by higher brine saturations downdip from the borehole and the potential for subsequent impacts on contaminant migration. To incorporate the effects of uncertainty in each case (E1 updip, E1 downdip, and undisturbed), a Latin hypercube sample size of 20 was used, for a total of 60 simulations. To assess the sensitivity of system performance on formation alteration of the DRZ, conditional CCDFs of

normalized contaminated brine releases were constructed and compared with the corresponding baseline model conditional CCDFs that were computed with constant DRZ permeability and porosity values. Based on comparisons between conditional CCDFs, computed releases to the accessible environment were determined to be essentially equivalent between the two treatments.

Preliminary performance assessments considered alternative conceptual models that allowed for some lateral extent of the DRZ into the halite surrounding the waste disposal region and for the development of a transition zone between anhydrites a and b and MB 138 (~~WIPP Performance Assessment Department~~ ***SNL*** 1993, Figures 4.1-2 and 5.1.2; Davies et al. 1993; Gorham et al. 1992). The transition zone was envisioned as a region that had experienced some hydraulic depressurization and perhaps some elastic stress relief because of the excavation, but probably no irreversible rock damage and no large permeability changes. Modeling results indicated that including the lateral extent of the DRZ had no significant effect on fluid flow. Communication vertically to MB 138 was ***thought to be*** a potentially important process, however, and the model adopted for the performance assessment ~~conservatively~~ assumes that the DRZ extends upward to MB 138 ***and permeability is sampled over the same range used in the 1997 PAVT.*** ~~without an intervening transition zone.~~

MASS-13.5 Actinide Transport in the Salado

The purpose of this model is to represent the transport of actinides in the Salado. ***The model for actinide transport in the Salado is implemented in the code NUTS.*** This model is also discussed in Section 6.4.5.4 ***and Appendix PA, Section PA-4.3***.

Actinide transport in the Salado is conceptualized as occurring only by advection through the porous medium described in the Salado hydrology conceptual model. Advection is the movement of material with the bulk flow of fluid. Other processes that might disperse actinides, such as diffusion, hydrodynamic dispersion, and channeling in discrete fractures, are not included in the conceptual model.

Advection is a direct function of fluid flow, which is discussed in the conceptual model for Salado fluid flow.

This application of NUTS treats the transport of radionuclides within all the regions for which BRAGFLO computes brine and gas flow. The brine must pass through some part of the repository at some period in its history to become contaminated. While there, it is assumed to acquire radioactive constituents, which it then transports by advection to other regions outside the repository. NUTS uses BRAGFLO's velocity field, pressures, porosities, saturations, and other model parameters (including geometrical grid, residual saturation, material map, brine compressibility, and time step) averaged over a given number of time steps (20 for this performance assessment calculation), which it takes as input for its transport calculations. Consequently, the results of NUTS are subject to all the uncertainties associated with BRAGFLO's conceptual model and parameterization, which will not be repeated here. Details of the source term are discussed in Appendix ***PA, Attachment*** SOTERM.

This application of NUTS disregards sorptive and other retarding effects throughout the entire flow region, even though retardation must occur at some level within the repository, the marker

beds, and the anhydrite interbeds, and especially in zones with clay layers or clay as accessory minerals.

This application of NUTS neglects molecular dispersion, which leads to uncertainty. For materials of interest in the WIPP repository system, molecular diffusion coefficients are at a maximum on the order of 4×10^{-10} ~~square meters~~ ***m^2*** per second. Thus, the simplest scaling argument using a time scale of 10,000 years leads to a molecular diffusion (that is, mixing) length scale of approximately 33 ~~feet~~ ***ft*** (10 m~~eters~~), which is negligible compared to the lateral advection length scale of roughly 7,874 ~~feet~~ ***ft*** (2,400 m~~eters~~) (the lateral distance from the repository to the accessible environment).

This application of NUTS also neglects mechanical dispersion, which leads to additional uncertainty (see Section 6.4.5.4.2). Dispersion is quantified by dispersivities, which are empirical (tensor) factors that are proportional to flow velocity (to within geometrical factors related to flow direction). They account for both the downstream and cross-stream spreading of local extreme values in concentration of dissolved constituents. Physically, the spreading is caused by the fact that both the particle paths and velocity histories of once-neighboring particles can be vastly different because of material heterogeneities characterized by permeability variations. These variations arise from the irregular cross-sectional areas and tortuous nonhomogeneous, nonisotropic connectivity between pores. Because of its velocity dependence, the transverse component of mechanical dispersivity tends to transport dissolved constituents from regions of relatively rapid flow (where mechanical dispersion has a larger effect) to regions of slower flow (where mechanical dispersion has a smaller effect). In the downstream direction, dispersivity merely spreads constituents in the flow direction. Conceptually, ignoring lateral spreading assures that dissolved constituents will remain in the rapid part of the flow field, which assures their transport toward the boundary. Similarly, ignoring longitudinal dispersivity ignores the elongation of a feature in the flow direction, which ignores foreshortening (or lengthening) of arrival times. However, because the EPA release limits are time-integrated measures, the exact times of arrival are unimportant for constituents that arrive at the accessible environment within the assessment period (10,000 years).

Advection is therefore the only transport mechanism considered important, which underscores NUTS' reliance on BRAGFLO. Because the Darcy flows are given to NUTS as input, the maximum solubility limits for combined dissolved and colloidal components are the most important NUTS parameters. ***These components*** ~~They~~ are described in Appendix ***PA, Attachment*** SOTERM ~~(Section SOTERM.7)~~.

MASS-14.*0* GEOLOGIC UNITS ABOVE THE SALADO

The model for geologic units above the Salado was developed to provide a reasonable and realistic basis for simulations of fluid flow within the disposal system and detailed simulations of groundwater flow and radionuclide transport in the Culebra. The conceptual model for these units is also discussed in Section 6.4.6~~)~~ of this application.

The conceptual model used in ~~performance assessment~~ ***PA*** for the geologic units above the Salado is based on the overall concept of a groundwater basin, as introduced in Chapter 2.0

(Section 2.2.1.1) of this ***recertification*** application, and developed further in ***CCA Appendix MASS,*** Section MASS.14.2. The computer code SECOFL3D was used to evaluate the effect on regional-scale fluid flow by recharge and rock properties in the groundwater basin above the Salado ***(CCA Appendix MASS, Attachment 17-2)***. However, simpler models for this region are implemented in codes used in performance assessment. For example, in the BRAGFLO model, layer thicknesses, important material properties including porosity and permeability, and hydrologic properties such as pressure and initial fluid saturation are specified, but the model geometry and boundary conditions are not suited to groundwater basin modeling (nor is the BRAGFLO model used to make inferences about groundwater flow in the units above the Salado). In ***PA*** ~~performance assessment~~ the Culebra is the only subsurface pathway modeled for radionuclide transport above the Salado, although the groundwater basin conceptual model includes other flow interactions. The Culebra model implemented in ***PA*** ~~performance assessment~~ includes spatial variability in hydraulic conductivity and uncertainty and variability in physical and chemical transport processes. Thus, the geometries and properties of units in the different models applied to the units above the Salado by the DOE are chosen to be consistent with the purpose of the model.

~~The groundwater basin model incorporated into the code SECOFL3D is the most general and least limited model available to the DOE for investigating how fluid flow in the units above the Salado is affected by variation in regional rock properties, basin geometries, and boundary conditions (including recharge changes and climate change). This code is used for calculations in support of this application but not in performance assessment per se. Studies performed with this code provide support for the performance assessment assumption of a confined Culebra and quantify the possible effects of future change in climate on the performance of the WIPP.~~

The ***MODFLOW-2000*** ~~SECOFL2D~~ and SECOTP2D codes are used directly in ~~performance assessment~~ ***PA*** to model fluid flow and transport in the Culebra. The assumptions made in these codes are discussed in Section 6.4.6.2 and Section MASS-15***.0***.

With respect to the units above the Salado, the BRAGFLO model is used only for determination of fluid fluxes between the shaft or intrusion borehole and hydrostratigraphic units. For this purpose, it does not need to resolve regional or local flow characteristics.

The basic stratigraphy and hydrology of the units above the Salado are described in Sections 2.1.3.5 through 2.1.3.10, and Section 2.2.1.4, respectively. Additional supporting information is contained in ***CCA*** Appendices GCR, HYDRO, and SUM. Details of the conceptual model for each unit are described in Sections 6.4.6.1 through 6.4.6.7.

MASS-14.1 Historical Context of the Units above the Salado Model

See CCA Appendix MASS, Section MASS.14.1 for historical information relating to the conceptual models for units above the Salado for the CCA. The conceptual models for the units above the Salado are unchanged for CRA-2004. However, CRA-2004 uses MODFLOW-2000 in place of SECOFL2D to model fluid flow in the Culebra.

~~The model used in the WIPP FEIS in 1980 (documented in Lappin et al. 1989, Table 1-1, 1-14 to 1-16) recognized three water-bearing zones within the Rustler, that is, the Magenta, Culebra, and~~

~~the Rustler-Salado interface (Lappin et al. 1989, 7 – 87). The Culebra and Magenta, although known to be separate units, were combined for regional-scale transport modeling into a Rustler aquifer and assigned a uniform hydraulic conductivity, except in Nash Draw. In the modeling, the Rustler aquifer was assumed to be an isotropic porous medium with a uniform porosity of 0.10 (Lappin et al. 1989, Table K-2, K-18). Regional flow was assumed to be toward the southwest, with discharge at Malaga Bend on the Pecos River. Numerical modeling was not able to consider the possible impact of variations in brine density within the Rustler; instead, modeling used an equivalent freshwater head. Steady-state flow directions and rates were assumed. Fluid flow in units above the Rustler was not considered because the limited available information suggested that these units were unsaturated. Units below the Castile were assumed to have no effect on performance and were not included in the analysis.~~

~~Several developments had taken place by 1989 (Lappin et al. 1989). Most importantly, interest in fluid flow within the Rustler became strongly focused on the Culebra. The Culebra is at least one order of magnitude more permeable than the Magenta, except in Nash Draw. Modeling by Barr et al. (1983) showed no potential for significant transport or fluid movement through the Magenta, and none of the hydraulic tests in the Magenta shows anything but porous-medium behavior. All other units within the Rustler (unnamed lower member, Tamarisk, Forty-niner) were even less permeable than the Magenta. Testing at DOE-2 had shown that permeability of the lower Dewey Lake was significantly lower than in the Magenta (Beauheim 1986). In the Draft Supplemental Environmental Impact Statement (DSEIS) (DOE 1989) and the December 1992 preliminary performance assessment calculations, all fluid flow and transport was assumed to be concentrated in the Culebra; this was thought to be a conservative approach because it did not allow flow in units in which release to the accessible environment was not possible.~~

~~Other important changes were in place by 1989. The potential for vertical fluid flow within the Rustler was recognized, on the basis of limited data, although for flow and transport calculations, the Culebra was assumed to be perfectly confined. Long-term flow transients within the system, related to climate change, were considered to be likely. Finally, the possibility of vertical fluid flow in an open borehole between the Rustler and the Bell Canyon was considered, but it was concluded that such fluid flow would be directed downward and was therefore of no physical or regulatory concern (Lappin et al. 1989).~~

~~Use of the groundwater basin conceptual model to gain an understanding of regional flow in the units above the Salado was initiated in a modeling study performed by Davies (1989). He selected boundaries to coincide with hydrologic features and used geologic data to infer hydraulic conductivity values for areas in which conductivity measurements were not available. Recognizing the three-dimensional nature of the regional groundwater system, Davies oriented two-dimensional simulations in both vertical and horizontal planes. The vertically oriented simulations were performed because it was recognized that the transient nature of the system is related to movement of the water table and the consequent change in the amount of water stored in the rocks. Davies confirmed that the hypothesis that the modern-day flow system might be a transient response to recharge during the last glacial pluvial period (Lambert 1987; Lambert and Carter 1987; Lambert and Harvey 1987) is physically possible. He also concluded that as much as 25 percent of the total inflow to the Culebra could be entering as vertical flux, and that fluid pressures in the Culebra are less than hydrostatic because the Culebra is well connected to the discharge area and poorly connected to the source of recharge. He suggested that the results of~~

~~his study could be expanded by, among other things, using a fully three-dimensional approach and additional study of the role of long-term transient changes in flow.~~

~~As a first step in extending the work of Davies, Corbet and Wallace (1993) developed a fully three-dimensional model with an adaptive upper boundary condition to approximately simulate movement of the water table. These simulations were performed using a version of the United States Geological Survey (USGS) code MODFLOW (McDonald and Harbaugh 1988) that was modified to include seepage faces. The modified MODFLOW model was limited in its capabilities in that it only approximately calculated the position of the water table and did not account for lateral variations in hydraulic conductivity. Nonetheless, the simulation results provided the first information about possible recharge rates at a regional scale and the sensitivity of groundwater flow patterns to changes in recharge. Specifically, the results suggested that rates of recharge to the saturated zone do not exceed several millimeters per year and that flow patterns in confined units are sensitive to small changes, perhaps only a few tenths of a millimeter per year, in rates of recharge.~~

~~A new numerical code, SECOFL3D (Knupp 1996), was used to perform the most recent three-dimensional simulations (Corbet 1994; Corbet and Swift 1996 [see Attachment 17-1]). The algorithm implements a rigorous treatment of the free-surface and seepage-face boundary conditions (Bear and Verruijt 1987; Dagan 1989; de Marsily 1986) and is designed to be robust even if extremely large contrasts in hydraulic conductivity are present within the model domain. A moving mesh that adaptively deforms so that its upper surface conforms to the moving water table is used to ensure that the entire computational domain remains saturated.~~

MASS-14.2 Groundwater-Basin Conceptual Model

For a discussion on the groundwater-basin conceptual model, see CCA Appendix MASS, Section MASS.14.2.

~~The conceptual model that emerged from taking a groundwater-basin approach represents a significant advance in understanding (Section 2.2.1.1). It differs from previous conceptual models in that it includes a description of the geometry of the groundwater basin, the distribution of rock hydraulic properties, and the physical mechanisms that drive groundwater flow. Previous conceptual models were limited to describing current flow conditions. They provided little basis to extrapolate backward or forward in time or to predict the impact of human-induced disturbances to the hydrologic system.~~

~~An objective of groundwater basin modeling was to use numerical simulations to enhance conceptual understanding of the hydrogeology of the Culebra in the context of regional groundwater flow (Corbet and Knupp 1996). A conceptual model is considered to be a qualitative description of the hydrologic processes, the geometry of the hydrogeologic system, the hydrostratigraphy, and the pattern of groundwater flow. In short, a conceptual model is an interpretation of reality. The rest of this section presents aspects of the conceptual model of groundwater flow in the Culebra that was formulated by integrating the previous conceptual understanding with the new information that these numerical simulations provided. Simulation results are incorporated without specifically identifying them as such.~~

~~Groundwater flow in the Culebra in the vicinity of the WIPP is a portion of a larger hydrologic system that includes the rock units that overlie the Salado. This system extends laterally well beyond the WIPP site to the boundaries of a groundwater basin. The basin boundary is not fixed in time; the basin is more extensive during dry periods in which the water table is at depth and less extensive during wet periods in which the water table is near to the land surface. The boundaries of the numerical model (Figure 2-29 in Chapter 2.0) approximately represent the basin boundaries for dry periods. These boundaries, therefore, outline the minimum region that must be considered to conceptually understand the evolution of modern-day flow conditions and their extrapolation into the future.~~

~~There is a continuous water table across the groundwater basin. It is probably in the Dewey Lake within the WIPP-site boundary. In places the hydraulic conductivity of the Dewey Lake is small enough that groundwater inflow to an open drill hole penetrating the saturated portion of this unit is too slow to be easily observed. It is also possible that some saturated portions of the Dewey Lake might be perched, that is, that they overlie an unsaturated region. Perched regions, if they exist, are part of the percolation process. They might affect the distribution of percolation at the water table but do not directly affect flow in the saturated zone.~~

~~A fundamental aspect of the conceptual model that has evolved from groundwater basin modeling is that the groundwater system is dynamic and is responding to the drying of the climate that has occurred since the end of the Pleistocene. Recharge rates at the end of the Pleistocene were sufficient to maintain the modeled water table near the land surface over much of the model domain. Groundwater flow, at that time, was controlled by the intermediate features of the land-surface topography. The gentle east to west slope of the land surface in the vicinity of the WIPP, for example, caused groundwater in the Culebra to flow toward and discharge into Nash Draw. As the amount of moisture available to recharge the groundwater system decreased after the last glacial pluvial period, the elevation of the water table declined. The decline occurred first in areas of high topography. As the water table dropped, groundwater flow began to increasingly reflect the land-surface topography at the scale of the entire groundwater basin. That is, the flow was away from the areas along the north and north-east boundaries of the basin where land-surface elevations are greater than 3,609 feet (1,100 meters) and toward areas below 2,789 feet (850 meters) in the Pecos River valley along the south boundary of the basin.~~

~~Dissolution of the upper Salado and associated processes has generated a zoned distribution of hydraulic conductivity at the basin scale. Hydraulic conductivities in the region in which dissolution is assumed to have disrupted stratigraphic layering (zone 1 of Figure MASS-3 MASS-7) are orders of magnitude larger than the region in which the strata are intact (zone 4). A transition interval separates these regions. Flow magnitudes and directions are quite different in these regions. Lateral flow in the intact strata is slow and, regardless of the elevation of the water table, is directed toward the disrupted region in areas that are within about a kilometer of the transition interval. In contrast, flow in the disrupted region is relatively rapid and its direction depends on the elevation of the water table. Flow is toward topographic depressions along the west and south boundaries of the model domain if the water table is near the land surface. Flow is directed toward the portion of the Pecos River valley along the south boundary if the water table is at depth.~~

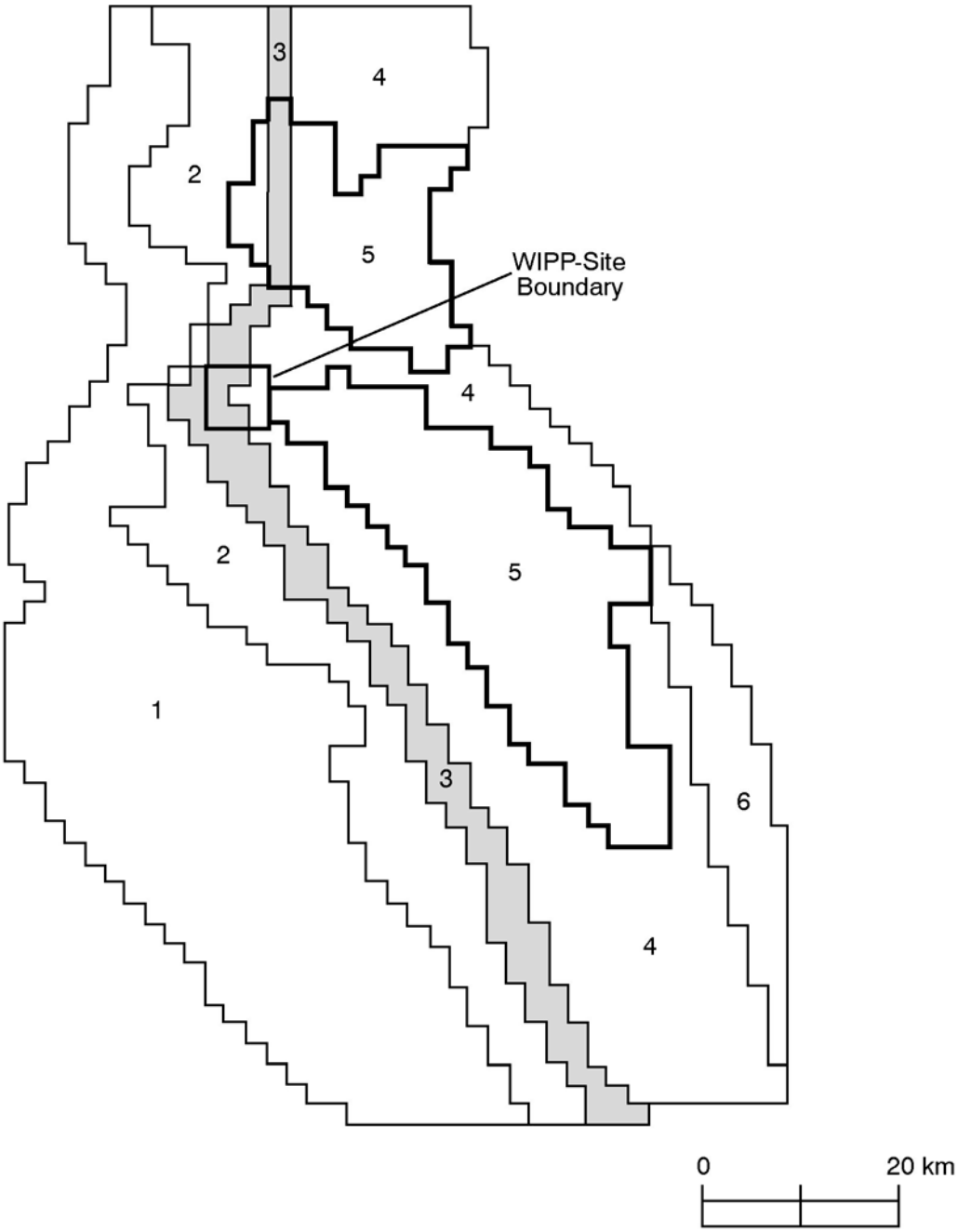

NOTE: Zonation approach used to represent the effects of depositional setting and post-depositional processes. Zone 1 ia a region in which dissolution of the upper Salado has fractured and disrupted overlying strata to the extent that stratigraphic layering is not preserved over long distances. In Zone 2, dissolution of the upper Salado is thought to have fractured the Rustler, but did not disrupt layering. Fractures that predate dissolution of the upper Salado are mostly filled with gypsum. These fracture fillings have been removed in Zone 3. Zone 4 represents intact strata. The region occupied by the halite facies of the mudstone/halite layers is indicated by Zone 5. A graben structure is shown as Zone 6.

CCA-MAS001-0

~~Figure MASS-3. Zonation Approaches Used in SECOFL3D Studies of Regional Groundwater Flow~~

~~Within the region of intact strata, the contrast in hydraulic conductivities plays an important role in determining flow patterns. The Dewey Lake and Triassic rocks are more permeable than the anhydrites at the top of the Rustler. Consequently most of the water that recharges the groundwater basin flows only in these rocks above the Rustler. The rest leaks vertically through the upper anhydrites and is available for flow through the rest of the Rustler. Gradients of hydraulic head along the base of the Dewey Lake provide the driving force for flow in the Rustler.~~

~~Groundwater flow in the Rustler is characterized by very slow vertical leakage through confining units and faster lateral flow in conductive units. Specific discharges (flow rates per unit area) in the Culebra are two to three orders of magnitude greater than the vertical specific discharges across the top of the Culebra. However, vertical leakage can contribute a significant portion of the total inflow to portions of the Culebra that are extensive enough that the upper surface is very much larger than the area available for lateral flow. It is difficult to quantify the relative contribution of vertical leakage because the hydraulic conductivity of the anhydrite confining layers at a regional scale is not well known.~~

~~As discussed in Chapter 2.0 (Section 2.2.1.4.1.2), studies of the isotopic composition of groundwater above the Salado (for example, Chapman 1986, 1988; Siegel et al. 1991) have generated debate about where and when the groundwater that is currently in the Culebra within the WIPP site was recharged. Conceptually, the sites of recharge can be found in a groundwater basin model by tracing various flowpaths from the WIPP site upstream to the water table. Flow paths were not identified as such as part of the simulation study, but some understanding can be reached by examining a large number of velocity distributions for the Culebra, Magenta, and Dewey Lake and Triassic units. These results suggest that flowpaths would have reached the water table in areas that are north and northeast of the WIPP site. The various flowpaths to the WIPP site would include relatively rapid lateral flow in the conductive units and slow vertical flow through the Rustler confining units. Flow paths that enter the WIPP site portion of the Culebra by vertical leakage across its upper surface originated outside of the WIPP site but closer to the WIPP site than the flow paths that enter the WIPP site by lateral flow within the Culebra. None of the water in the Culebra within the WIPP site is conceptualized as having been recharged in areas where the Culebra is at or near to the land surface. It is also noted that the travel times along the various flowpaths to the Culebra probably vary greatly. Therefore, the water currently in the Culebra is a mix of water with much different residence times.~~

~~The modern-day pattern of groundwater flow has not equilibrated to the present climate. There are two aspects to this disequilibrium. First, the position of the water table has not yet adjusted to past changes in recharge rates. A decrease in recharge that started at the end of the Pleistocene was complete by 8,000 years ago. The water table, however, is still in the process of adjusting to this change in recharge. Second, hydraulic heads in rocks with small conductivities are not adjusted to the current position of the water table. The base-case transient simulation shows, for example, that closed regions of maximum head occur in the Culebra at the present time. These maxima are in regions where the Culebra's conductivity is believed to have been reduced by precipitation of halite in pore space. Groundwater flows out of these regions too slowly for heads to remain in equilibrium with a falling water table. The persistence of these regions of high head delays the transition of the flow field to one that fully reflects the basin-scale topography.~~

~~The slow response of the water table to long-term changes in recharge is the dominant aspect of the transient nature of the groundwater system. However, superimposed on long-term changes in the flow system are short-term changes caused by alternating wet and dry periods during the Holocene. Each wet-and-dry cycle results in a rise and fall of the water table. The amount of change in the water table depends on the peak recharge rate and the rock properties. The simulated change is typically 16 to 49 feet (5 to 15 meters). Changes in hydraulic head in the Culebra lag behind changes in the water table and have a smaller amplitude. The overall effect of the Holocene wet periods is to slow the long-term decline of the water table and to superimpose short-term, and relatively small, variations to long-term flow velocities.~~

~~The new contributions to the conceptual understanding of the regional hydrogeology of the Culebra resulting from modeling from a groundwater basin perspective include the following:~~

- ~~The shape and elevation of the water table largely determine rates and directions of groundwater flow in the Culebra.~~

- ~~Groundwater inflow to the portion of the Culebra within the WIPP site boundary is by a combination of lateral flow within the Culebra and extremely slow vertical leakage from the overlying Tamarisk.~~

- ~~The term recharge refers to a process that occurs at the water table. The inflow to the Culebra originated as recharge distributed over large areas of the groundwater basin. Recharge that eventually reaches the Culebra within the WIPP site does not occur where the Culebra crops out or where overlying confining units have been removed or fractured. The paths that water follows as it flows from the water table to the Culebra at the WIPP site necessarily include vertical leakage across confining layers. The travel time to reach the Culebra varies greatly along the various paths. The travel times are probably thousands or tens of thousands of years.~~

- ~~Climate change alters recharge rates. Consequently the position of the water table changes and groundwater velocities at depth adjust accordingly.~~

- ~~Modern-day flow velocities in the Culebra at the WIPP site can be understood and simulated using the groundwater basin conceptual model. The generally north-to-south flow is a result of the modern-day depth of the water table and the basin-scale distribution of hydraulic conductivity. Flow in wetter climates would rotate toward Nash Draw to the west. Flow in the Culebra directed away from Nash Draw is not supported by this model.~~

- ~~The size and shape of the hydrogeologic system that determines groundwater flow velocities in the Culebra at the WIPP site have been tentatively identified.~~

MASS-15.*0* CULEBRA

The conceptual model for groundwater flow in the Culebra (a) provides a reasonable and realistic basis for simulating radionuclide transport in the Culebra and (b) allows evaluation of the extent to which uncertainty about groundwater flow in the Culebra may contribute to uncertainty in the

estimate of cumulative radionuclide releases from the disposal system. See ~~Chapter 6.0 (~~Section 6.4.6.2~~),~~ for additional references to other relevant discussions on this conceptual model.

The conceptual model used in performance assessment for groundwater flow in the Culebra treats the Culebra as a confined two-dimensional aquifer with constant thickness and spatially varying transmissivity (see ***CCA Appendix MASS,*** Attachment 15-7). Flow is modeled as single-phase (liquid) Darcy flow in a porous medium.

Basic stratigraphy and hydrology of the units above the Salado are described in Chapter 2.0***,*** ~~(~~Sections 2.1 and 2.2~~)~~. Additional supporting information is contained in ***CCA*** Appendices GCR, HYDRO, and SUM.

The conceptual model for flow in the Culebra is discussed in ~~Chapter 6.0 (~~Section 6.4.6.2~~)~~. Details of the calibration of the ~~transmissivity~~ ***T-***field***s***, based on available field data, are given in Appendix ***PA, Attachment*** TFIELD, ~~(~~Section TFIELD-4~~)~~. Initial and boundary conditions used in the model are given in Section 6.4.10.2. A discussion of the adequacy of the two-dimensional assumption for ~~performance assessment~~***PA*** calculations is included as Attachment 15-7 ***to CCA Appendix MASS***.

The principal parameter used in the ~~performance assessment~~***PA*** to characterize flow in the Culebra is an index parameter (the transmissivity index) used to select a single ~~transmissivity~~ ***T-*** field for each Latin hypercube sample element from a set of calibrated fields, each of which is consistent with available data (see Appendix PAR~~, Parameter 35~~).

MASS-15.1 Historical Context of the Culebra Model

Since the FEIS in 1980, the model used to describe flow and transport within the Culebra has changed significantly. In the FEIS, the Culebra and Magenta were combined and modeled as one layer referred to as the Rustler aquifers. In the modeling, the Rustler aquifers were assumed to be an isotropic porous medium with a uniform porosity of 0.10 (Lappin et al. 1989, Table K-2, K-18). A uniform ~~transmissivity~~ ***T-***field was assumed across the model domain except in Nash Draw. Regional flow was assumed to be toward the southwest discharging at Malaga Bend on the Pecos River. (There was no regulatory framework or boundary defined at this time.) Numerical modeling was not able to consider the possible effect of variations in brine density within the Rustler, so modeling used an equivalent freshwater head. Steady-state flow directions and rates were assumed. As for physical-transport characteristics, the Culebra was incorporated into the Rustler aquifers and assumed to be an isotropic, homogeneous porous medium.

Haug et al. (1987) calibrated a flow model to the H-3 pumping test (Beauheim 1987a) and the effects from the excavation of the shafts. Data from numerous new boreholes installed and tested since the 1980 study were included in this model. The boundaries of the model were not much larger than the extent of the WIPP site. Brine densities were also used as a calibration target. The brine densities were assigned at the boundaries and subsequently modified to match the observed fluid densities. Vertical leakage was included in an attempt to calibrate the brine densities. This attempt led to the recommendation that future modeling studies treat the Culebra as a leaky-confined aquifer. The ~~transmissivity~~ ***T-***field was estimated by kriging and modified by the addition of pilot points, which were located by trial and error. In this model, single- and

double-porosity effects on the flow field were investigated. At the regional scale, the use of a double-porosity vs. single-porosity (matrix-only) conceptual model had little effect on the flow field.

A modeling study (LaVenue et al. 1990) conducted to support the DSEIS only slightly modified the conceptual model used by Haug et al. (1987). The differences in the conceptual model were the assumptions that brine density varied spatially but was held constant through time, and vertical leakage was not included. It was assumed that the brine concentrations could be considered to have changed little over the period of time modeled. The boundaries of the 1989 study were much larger than those of the 1987 study, extending approximately 18.6 mi~~les~~ (30 ~~kilometers~~ ***km***) north and south and 12.4 mi~~les~~ (20 ~~kilometers~~ ***km***) in east and west. The model grid was centered on the WIPP site. The boundaries were selected to include the region for which head data were available and to minimize the boundary effects during transient simulation of the H-3, WIPP-13, and H-11 pumping tests. Fixed heads were assigned around all four boundaries based upon the regional head values. Transmissivities were estimated by kriging and ranged over seven orders of magnitude in this study. Pilot points were added to modify the ~~transmissivity~~ ***T-***field during steady-state and transient calibration. Pilot-point locations were selected using an adjoint sensitivity analysis technique. The Culebra ~~transmissivity~~ ***T-***field ***were*** ~~was~~ calibrated on the basis of 41 test locations. Transmissivity was recognized to vary by approximately three orders of magnitude within the WIPP site. Modern flow in Culebra was recognized as being predominantly north to south on the WIPP site, and strongly affected by a high-transmissivity zone in the southeastern portion of the WIPP site. Flow was calculated on the basis of a fully confined Culebra and boundary conditions applied at the WIPP site scale. As discussed in Lappin et al. (1989), local flow and transport behavior were affected by fracturing where the transmissivity is greater than approximately 10^{-6} ~~square meters~~ m^2 per second. For physical transport, a double-porosity (matrix-diffusion) transport model for off-site transport from waste panels was assumed. Transport parameters were based on best estimates from nonsorbing tracer tests at three locations (Jones et al. 1992). It was assumed that the effective thickness was equal to the total thickness. Contaminant-transport calculations were one-dimensional.

The initial conditions for the Culebra flow field have been taken from the hydrographs of the WIPP boreholes. Prior to excavation of the salt handling shaft, the hydrographs showed little evidence of head change over the ten years preceding the shaft excavations. Head values were selected for each borehole with a hydrograph that preceded shaft excavation or that was located far from the shaft effects on the flow field. These data provided an estimate of the undisturbed head field and were subsequently used as initial conditions for the Culebra model's transient simulation.

In modeling the hydrologic characteristics of the Culebra, SNL (1992-1993) generated multiple ~~transmissivity~~ ***T-***field conditioned on hydraulic test data (point transmissivity data and transient head data) and then sampled those fields. This procedure addressed uncertainties in the location-specific values of the Culebra transmissivity. The geologic conceptual model was further revised to indicate that the degree of fracture flow was related to the degree of gypsum cement in the fractures. Contaminant-transport calculations were two-dimensional. The effective thickness of the Culebra was taken to be equal to the total thickness. A range of physical-transport parameters was used, as opposed to best estimates, to address the variability of physical-transport

properties within the Culebra. The maximum fracture spacing was assumed to be equal to the total thickness of the Culebra (approximately 26 ~~feet~~ ***ft*** [8 m~~eters~~]). The fracture spacing used in modeling was a convenient modeling simplification based on the concept of through-going parallel fractures. Representing fracturing in terms of fracture spacing is a mechanism to ensure that the proper surface-to-volume ratios are used in estimating the role of matrix diffusion. Calculations considered the possibility of both single-porosity (fracture-flow-only) and double-porosity (matrix diffusion) behavior.

The main differences between the 1989 and 1992 models were the model boundary locations, boundary conditions, and the geostatistical approach used to develop and modify the ~~transmissivity~~ ***T-***field (LaVenue and RamaRao 1992). The 1992 model boundaries were rotated 38 degrees east to align with the axis of Nash Draw. This permitted the specification of a no-flow boundary condition along a portion of the western boundary, which was selected to coincide with the axis of Nash Draw. In addition, the northeastern corner of the model was treated as a no-flow boundary because of the low transmissivities in the area and the lack of any nearby regional heads to provide boundary head estimates. Transmissivities were simulated by conditional simulation. Pilot points were automatically located and assigned transmissivity values using an optimization routine during steady-state and transient-state calibration.

By 1994, the model of the Culebra's hydrologic characteristics was unchanged from that of December 1992. For the physical-transport characteristics, double-porosity transport was assumed, but the base case had large fracture spacing, effectively the same as the Culebra thickness. A single block size was assumed in each realization. Calculations still assumed an effective thickness equal to the total thickness.

~~Since 1994~~***For the 1996 CCA***, the model of the Culebra's regional hydrologic characteristics ha***d***~~s~~ not changed ***from the 1994 model***, although additional large-scale information from pumping at H-19 and small-scale information at Water Quality Sampling Program (WQSP) wells ~~has been~~***was*** incorporated into the calibration. Existing borehole-transmissivity interpretations ~~have been~~***were*** refined. The model of the physical-transport characteristics ***were*** ~~has~~ changed on the basis of analysis of new data from H-19 and H-11 and reanalysis of previous tests of H-3, H-11, H-6. The Culebra ~~is now~~ ***was*** conceived of as a fractured porous medium with inherent local variability in the degree and scale of fracturing. Examination of core and shaft exposures ~~has~~ revealed that there are multiple scales of porosity within the Culebra including fractures from microscale to large, vuggy zones, and inter-particle and inter-crystalline porosity. This variability leads to both lateral and vertical variations in permeability. Advection is believed to occur largely through fractures; however, in some areas it may also occur through vugs connected by small fractures and interparticle porosity. Diffusion occurs into all connected porosity. ~~Performance assessment~~***PA***, rather than conceiving of transport in terms of fracture and matrix porosities, conceives the Culebra as being composed of advective and diffusive porosities. Matrix diffusion is still believed to be effective and significant. The effective transport thickness is thought to be less than the total stratigraphic thickness. The available data suggest that the permeability of the upper portion of the Culebra is relatively low. Therefore the DOE has concluded that the Culebra is adequately represented by a double-porosity continuum model on the scale of ~~performance assessment~~***PA*** calculations, and it is not necessary to use a discrete-fracture model on this scale.

For the 2004 PA, the method of defining the initial (pre-calibration) distribution of T within the Culebra has been revised to explicitly include the geologically zoned distribution of T first developed for the basin-scale model. Three zones are identified: an eastern zone in which halite is present in the Rustler members immediately above and/or below the Culebra and the Culebra transmissivity is consistently low (log T [m^2/s] < -5.4), a western zone in which dissolution of the upper Salado has occurred and the Culebra T is consistently high (log T [m^2/s] > -5.4), and an intermediate transition zone that includes most of the WIPP site. Areas of high T are distributed stochastically within 27.8 percent of the intermediate transition zone to represent the current uncertainty in their locations. Within each of the three zones, T is inversely correlated to the thickness of overburden above the Culebra.

The flow code used for the CRA T-fields was MODFLOW-2000 (Harbaugh et al. 2000). The model domain for CRA-2004 is similar in size (22.4 km [13.9 mi] wide by 30.7 km [19.1 mi] long) to that used for the CCA (approximately 22 km [13.7 mi] wide by 30 km [18.6 mi] long), but is oriented with the long axis extending north to south. The model domain was discretized into uniform 100-m [328-ft] by 100-m [328-ft] grid blocks. Constant-head conditions were prescribed for the eastern boundary of the model, as well as for the eastern portions of the northern and southern boundaries. Flow lines (no-flow boundaries) were prescribed from northeast to southwest down the axis of the northern part of Nash Draw, and from northwest to southeast down the southern arm of Nash Draw. Model cells in the northwest and southwest portions of the model domain beyond the flow lines were treated as inactive by MODFLOW-2000.

Implementation of the pilot-point method for T-field calibration was also revised for the CRA-2004 T-fields. Instead of using an adjoint-sensitivity approach to optimize the locations of the same number of pilot points as there were well locations, 100 pilot points were located to provide a relatively uniform distribution of wells and pilot points within the intermediate transition zone and near the borders of the other two zones. The regularization technique described by Doherty (2003) was used to prevent the large number of pilot points from causing numerical instability. PEST v. 5.5 (Doherty 2002) was used instead of GRASP to optimize T at pilot-point locations during the model-calibration process. The calibration process involved matching to heads measured in late 2000 and to transient heads at 40 wells resulting from seven major pumping tests.

Additional information on the T-field modeling performed for the 2004 PA is given in Chapter 6 and Appendix PA, Attachment TFIELD. Transport modeling for CRA-2004 was performed in the same manner as for the CCA.

MASS-15.2 Dissolved Actinide Transport and Retardation in the Culebra

The purpose of this model is to represent the effects of advective transport, physical retardation, and chemical retardation on the movement of actinides in the Culebra. This conceptual model is also discussed in Section 6.4.6.2.1.

The properties of the Culebra have been characterized by direct observation in outcrop, boreholes, and shafts (Holt and Powers 1984, 1986, 1988, 1990), field hydraulic testing and analysis (Beauheim 1987b), field tracer testing and analysis (Attachment 15-6; Jones et al. 1992;

Mercer and Orr 1979), and laboratory testing and analysis (Papenguth and Behl 1996a, 1996b). The conceptual model for dissolved actinide transport in the Culebra is based on these observations, tests, and analyses. ***Because testing and analysis of the Culebra suggest that its upper portion does not play a significant role in transport, transport is modeled only for the lower portion of the Culebra.***

The conceptual model for actinide transport in the Culebra has three principal components: advective transport, physical retardation, and chemical retardation. Two types of porosity are present—porosity in which advective transport occurs, and porosity that is relatively inactive in advective transport. This type of behavior is typically referred to as double porosity~~. Because testing and analysis of the Culebra suggest that its upper portion does not play a significant role in transport, transport is modeled only for the lower portion of the Culebra.~~

Advective transport refers to the transport of actinides in those pores of the Culebra where the principal fluid flow occurs. This flow primarily occurs in fractures, but may also occur in microfractures connecting vugs in vuggy regions or other portions of the porosity of the Culebra that contain large pore-throat apertures (that is, high permeability regions). This mechanism includes the effects of diffusion and dispersion in advective porosity as well as the movement of actinides with the bulk fluid flow. Advective transport is thought to be controlled by hydraulic gradient, hydraulic conductivity, ***formation*** thickness, and advective porosity.

Physical retardation refers to the process of diffusion from advective porosity into diffusive porosity, that is, those portions of the porosity of the Culebra that are relatively inactive in advective transport. Once in the diffusive porosity, the ***transport of*** actinides ~~are no longer carried along by the most rapidly moving liquids, and their rate of movement~~ is controlled by diffusion and sorption. Diffusion can be an important process for effectively retarding solutes by transferring mass from the porosity where advection (flow) is the dominant process into other portions of the rock. The properties that control the diffusion of actinides into the diffusive porosity are the surface-area-to-volume ratio ~~between~~***of the matrix blocks*** ~~advective porosity and the diffusive porosity~~, the tortuosity of the diffusive porosity, and ***actinide*** free-water diffusion coefficients (see ***CCA Appendix MASS,*** Attachment 15-3).

Chemical retardation refers to the sorption of actinides on minerals present in the Culebra. ~~The s~~***S***orption is thought to occur on dolomite grains, but will also occur on clay or other minerals. In the conceptual model, chemical retardation occurs only in the diffusive porosity, and adds to the effects of the physical retardation. The governing properties for sorption are described in a parametric expression of the degree to which dissolved actinides tend to sorb or remain in solution (in the mathematical model, a K_d ~~f~~or a linear isotherm is used), which requires the concentration of actinides in solution and the abundance of minerals on which sorption can occur (see ***CCA Appendix MASS,*** Attachment 15-1).

Advective porosity is thought to be a small percentage of the total volume of the Culebra ~~involved in transport~~. This porosity is interconnected and contains high-permeability features such as fractures or vuggy pore structures. In this advective porosity, little actual rock material is considered to exist (in other words, it is the fracture apertures and pore volumes without surrounding rock). In contrast, diffusive porosity makes up the major portion of the Culebra pore volume. It comprises lower-permeability features and most of the rock material. The rate

at which diffusion removes solutes from advective porosity is a function of the surface area-to-volume ratio ~~between~~***of*** the ***matrix blocks***~~advective and diffusive porosity~~. For a given geometry of advective porosity assumed in a model (for example, parallel-plate fractures), this surface area-to-volume ratio can be expressed as a characteristic length, which is known as the matrix block length (for example, the thickness of a matrix slab between two parallel-plate fractures).

In summary, the conceptual model for dissolved actinide transport in the Culebra includes two types of porosity: advective porosity associated with high-permeability features of the Culebra, and diffusive porosity associated with lower-permeability features. These two types of porosity are distributed throughout the Culebra and are intertwined on a small scale; hence, mapping their regional extent or boundaries between them is not feasible. Advection, diffusion, and dispersion of dissolved actinides occur within the advective porosity. Diffusion (physical retardation) and sorption (chemical retardation) occur within the diffusive porosity. Advective porosity makes up a small portion of the overall pore volume of the Culebra; diffusion is an important process for transferring ~~mass~~***actinides*** into other portions of the rock ~~mass where~~***in which*** there is a larger surface area for sorption. Because the upper portion of the Culebra has been observed to be relatively inactive in solute transport in tests, it is assumed to be unimportant and is not included in the conceptual model. Attachment 15-6 ***of CCA Appendix MASS*** contains additional information on the transport properties of the Culebra.

Several parameters are referred to or implied in the conceptual model as discussed in Section 6.4.6.2. For transport in advective porosity, the principal parameter is the porosity of the network, but because of links to the Culebra fluid flow model, the hydraulic gradient and hydraulic conductivity largely control the specific discharge calculated by ***MODFLOW-2000*** ~~SECOFL2D~~. Within diffusive porosity, the porosity, tortuosity, and diffusion coefficients for various actinides are important because of their effect on the rate of diffusion. A parameter called matrix block length, a measure of the surface area between the advective and diffusive porosities, is also important. The density of sorbing minerals and their sorption properties, expressed by K_d ~~(the distribution coefficient)~~, are important in chemical retardation.

It is commonly assumed that there should be a relationship between the conductivity of advective porosity and its porosity and distribution, that is, that the fracture permeability, porosity, and aperture or spacing should be correlated. Data collected and analyzed at the WIPP do not support this assumption. There are no meaningful trends among these parameters for the data that have been collected. Therefore, values of these parameters are not correlated in the ~~performance assessment~~***PA*** (see ***CCA Appendix MASS,*** Attachment 15-6, ***page*** 14 ***and*** Attachment 15-10).

Transport of actinides in the Culebra is coupled to several other conceptual models. An important coupling is to models for features that can introduce actinides to the Culebra, for example, the exploratory borehole, shafts and shaft seals, and dissolved actinide source term. The most important coupling is to the model for flow in the Culebra. Because transport in the Culebra is one of the last processes to occur along this pathway prior to release, it does not feed back to other conceptual models in any significant manner. ~~In a manner of speaking, t~~***T***his conceptual model falls at the downstream end of the overall disposal system model, and thus has little or no impact on models that come before it.